Electronic Supplementary Material (ESI) for Dalton Transactions.
This journal is © The Royal Society of Chemistry 2022

Electronic Supplementary Information

Experimental and Computational Tuning of Metalla-*N*-heterocyclic Carbenes at Palladium(II) and Platinum(II) Centers

Maria V. Kashina, Konstantin V. Luzyanin,* Eugene A. Katlenok, Alexander S. Novikov, and Mikhail A. Kinzhalov *

Table of content

S1. X-ray diffraction studies

Table S1. Crystal data and structure refinement for **11**, **16**, **18**.

Identification code	**11**	**16**	**18**
CCDC	2133432	2133435	2133433
Empirical formula	$C_{45}H_{48}Cl_2N_6Pt_2$	$C_{46}H_{47}N_9Pd_2S_2$	$C_{46}H_{47}N_9Pt_2S_2$
Formula weight	1133.97	1002.84	1180.22
Temperature/K	293(2)	297.2(2)	99.98(10)
Crystal system	triclinic	monoclinic	monoclinic
Space group	P-1	$P2_1/c$	$P2_1/c$
a/Å	7.50970(10)	8.2035(2)	8.08540(10)
b/Å	8.75810(10)	30.9219(8)	30.3986(3)
c/Å	33.6683(2)	18.7259(5)	18.7295(2)
α/°	92.1540(10)	90	90
β/°	90.2040(10)	98.347(3)	97.8860(10)
γ/°	92.1370(10)	90	90
Volume/Å^3	2211.26(4)	98.347(3)	4559.89(9)
Z	2	4	4
ρ_{calc}g/cm^3	1.703	1.417	1.719
μ/mm^{-1}	13.060	7.325	12.497
F(000)	1100.0	2040.0	2296.0
Crystal size/mm^3	0.08 × 0.06 × 0.02	0.1 × 0.06 × 0.04	0.06 × 0.14 × 0.19
Radiation	CuKα (λ = 1.54184)	CuKα (λ = 1.54184)	CuKα (λ = 1.54184)
2Θ range for data collection/°	5.254 to 124.996	5.56 to 134.996	5.58 to 119.984
Index ranges	$-9 \le h \le 9$, $-19 \le k \le 19$, $-36 \le l \le 38$	$-9 \le h \le 9$, $-34 \le k \le 37$, $-22 \le l \le 21$	$-9 \le h \le 8$, $-34 \le k \le 34$, $-21 \le l \le 20$
Reflections collected	44150	40403	71892
Independent reflections	7053 [R_{int} = 0.0405, R_{sigma} = 0.0241]	8447 [R_{int} = 0.0482, R_{sigma} = 0.0370]	8233 [R_{int} = 0.0543, R_{sigma} = 0.0230]
Data/restraints/parameters	7053/0/508	8447/0/544	8233/0/544
Goodness–of–fit on F^2	1.088	1.042	1.063
Final R indexes [I≥2σ (I)]	R_1 = 0.0344, wR_2 = 0.0805	R_1 = 0.0359, wR_2 = 0.0935	R_1 = 0.0212, wR_2 = 0.0493
Final R indexes [all data]	R_1 = 0.0362, wR_2 = 0.0815	R_1 = 0.0413, wR_2 = 0.0967	R_1 = 0.0218, wR_2 = 0.0498
Largest diff. peak/hole /e·Å^{-3}	3.69/-0.82	0.51/-0.75	0.77/-0.85

Table S2. Selected bonds and angles in crystal structure of **11**.

	Bond length, Å		Angle, °
Pt1–Cl1	2.3498(17)	N2–Pt1–Cl1	94.46(14)
Pt1–N2	2.038(5)	C1–Pt1–Cl1	172.41(17)
Pt1–C1	1.983(6)	C1–Pt1–N2	78.8(2)
Pt1–C8	1.924(6)	C8–Pt1–Cl1	84.4 (2)
Pt2–Cl2	2.3907(16)	C8–Pt1–N2	175.8(3)
Pt2–N1	2.054(4)	C8–Pt1–C1	102.6(3)
Pt2–C7	1.989(5)	N1–Pt2–Cl2	101.57(14)
Pt2–C36	1.912(7)	C7–Pt2–Cl2	177.86(18)
N2–C2	1.347(8)	C7–Pt2–N1	79.3(2)
N2–C6	1.350(8)	C36–Pt2–Cl2	81.0(2)
N1–C1	1.349(8)	C36–Pt2–N1	177.2(2)
N1–C2	1.398(7)	C36–Pt2–C7	98.0(3)
N3–C1	1.341(7)	C2–N2–Pt1	113.4(4)
N3–C7	1.449(8)	C6–N2–Pt1	125.4(4)
N3–C18	1.439(7)	C1–N1–Pt2	115.7(4)
N4–C7	1.264(8)	C2–N1–Pt2	130.6(4)
N4–C27	1.405(8)	N1–C1–Pt1	116.5(4)
N5–C8	1.136(8)	N3–C1–Pt1	129.5(4)
N5–C9	1.407(9)	N3–C1–N1	113.9(5)
N6–C36	1.145(8)	N3–C7–Pt2	111.5(4)
N6–C37	1.395(8)	N4–C7–Pt2	134.7(5)
		N5–C8–Pt1	168.7(6)
		N6–C36–Pt2	170.0(6)
		C2–N2–C6	120.5(5)
		C1–N1–C2	113.7(5)
		C1–N3–C7	118.6(5)
		C1–N3–C18	123.5(5)
		C18–N3–C7	117.7(5)
		C7–N4–C27	123.9(5)
		N4–C7–N3	113.7(5)
		C8–N5–C9	179.3(7)
		C36–N6–C37	178.0(8)
		N1–C2–C3	124.2(6)
		N2–C2–N1	116.3(5)
		N2–C2–C3	119.4(5)

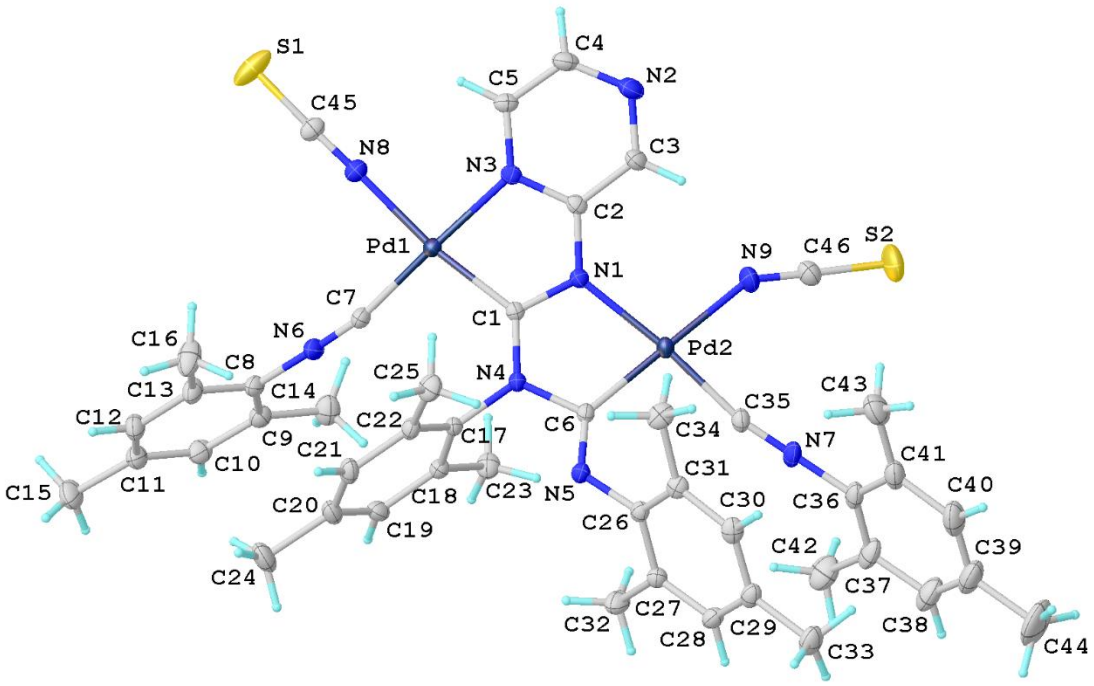

Figure S1. View of **16** with the atomic numbering schemes. Solvent molecule and hydrogen labels were omitted for simplicity.

Table S3. Selected bonds and angles in crystal structures of **16**, **18**.

	Bond length, Å			Angle, °	
	18	**16**		**18**	**16**
M1–C1	1.981(3)	1.986(3)	N2–M1–N8	93.17(10)	93.57(11)
M1–C7	1.936(3)	1.947(3)	C7–M1–N8	87.29(11)	87.07(12)
M1–N2	2.032(2)	2.018(2)	C1–M1–N2	78.66(10)	78.85(10)
M2–C6	1.982(3)	1.985(3)	C7–M1–C1	100.92(12)	100.65(12)
M2–C35	1.922(3)	1.951(3)	N1–M2–N9	99.23(10)	100.43(12)
M1–N8	2.031(3)	2.039(3)	C6–M2–N1	79.42(11)	79.58(10)
M2–N9	2.096(3)	2.104(3)	C35–M2–N9	84.67(12)	84.30(13)
N6–C7	1.140(4)	1.149(4)	C35–M2–C6	96.36(18)	95.62(12)
N7–C35	1.148(4)	1.146(4)	N6–C7–M1	168.9(3)	167.5(3)
C1–N1	1.357(4)	1.343(4)	C7–N6–C8	178.7(3)	178.0(4)
C5–N2	1.346(4)	1.339(4)	N7–C35–M2	173.1(3)	169.6(3)
C6–N4	1.461(4)	1.456(4)	C35–N7–C36	170.4(4)	172.5(4)
C6–N5	1.260(4)	1.250(4)	C46–N9–M2	147.1(3)	147.7(3)
N8–C45	1.151(4)	1.135(5)	C45–N8–M1	175.7(3)	178.5(3)
N9–C46	1.158(5)	1.152(5)			
C45–S1	1.619(3)	1.608(4)			
C46–S2	1.612(4)	1.611(5)			

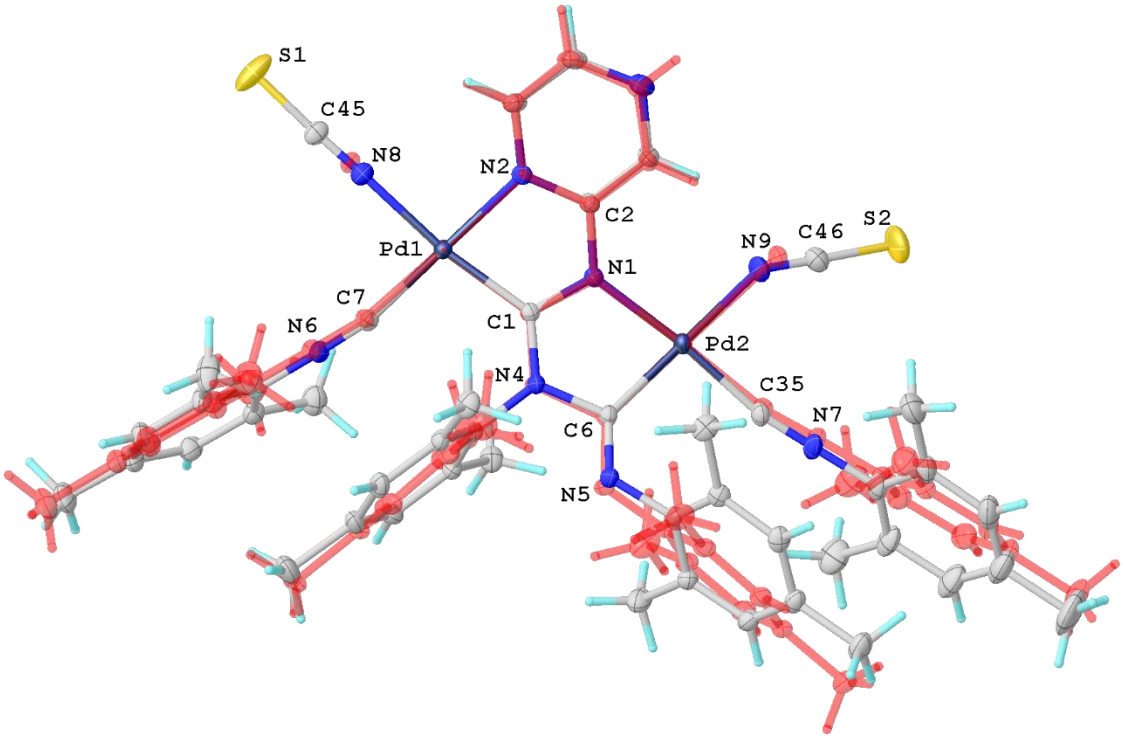

Figure S2. The view of overlaid **16** and **11** (red) structures with the selected atomic labels for **16**.

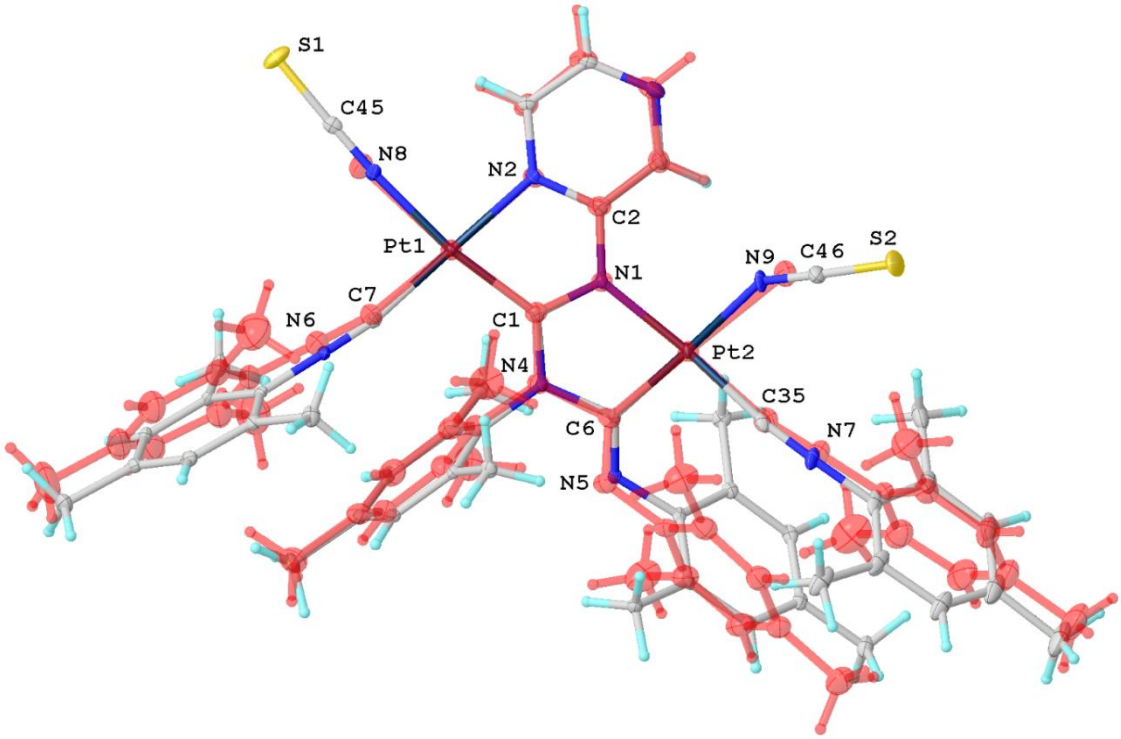

Figure S3. The view of overlaid **18** and **11** (red) structures with the selected atomic labels for **18**.

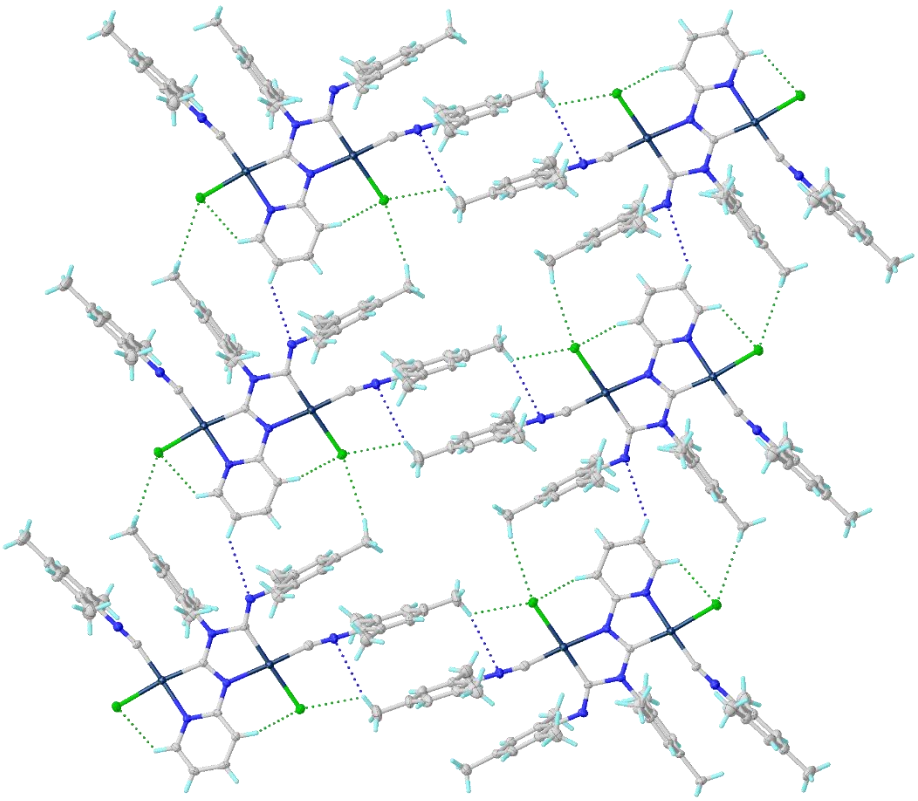

Figure S4. The crystal packing of complex **11**.

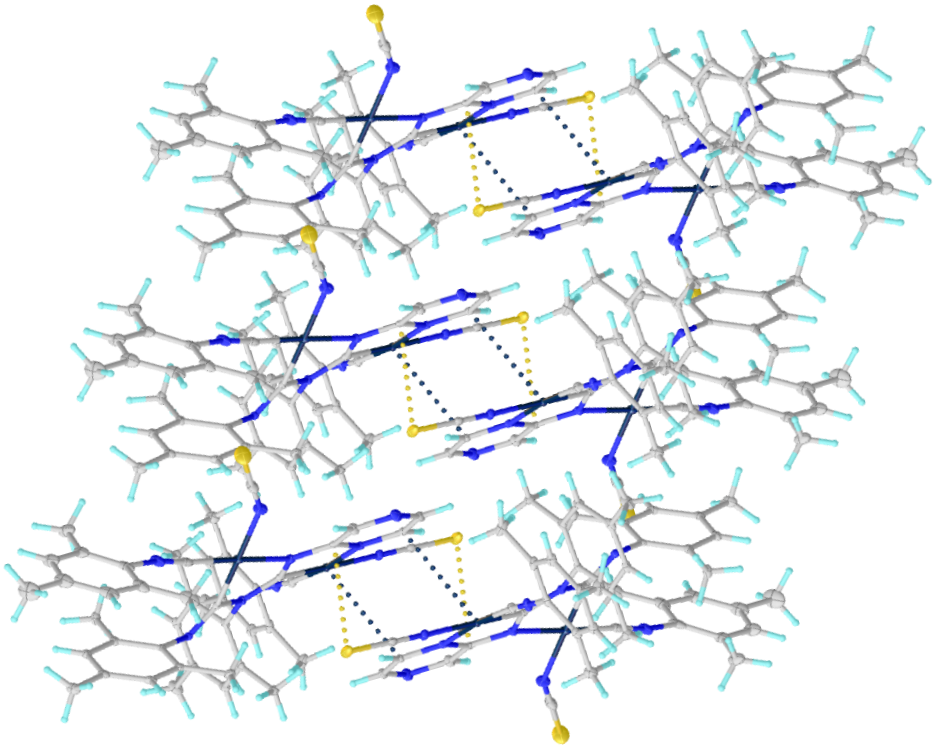

Figure S5. The crystal packing of complex **18**.

S2. UV-vis absorption spectra in KBr pellets

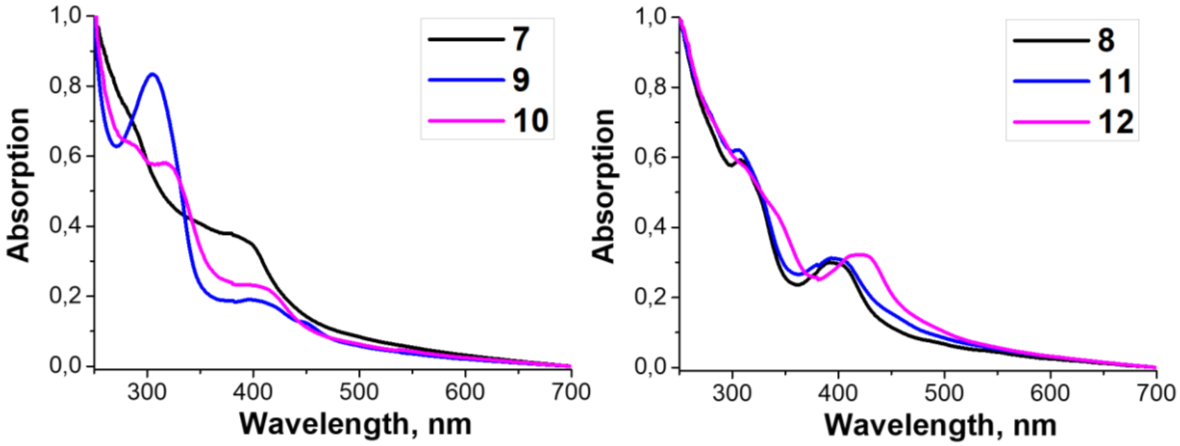

Figure S6. Normalized UV-Vis absorption spectra for **7**–**12** in solid state (KBr) at RT.

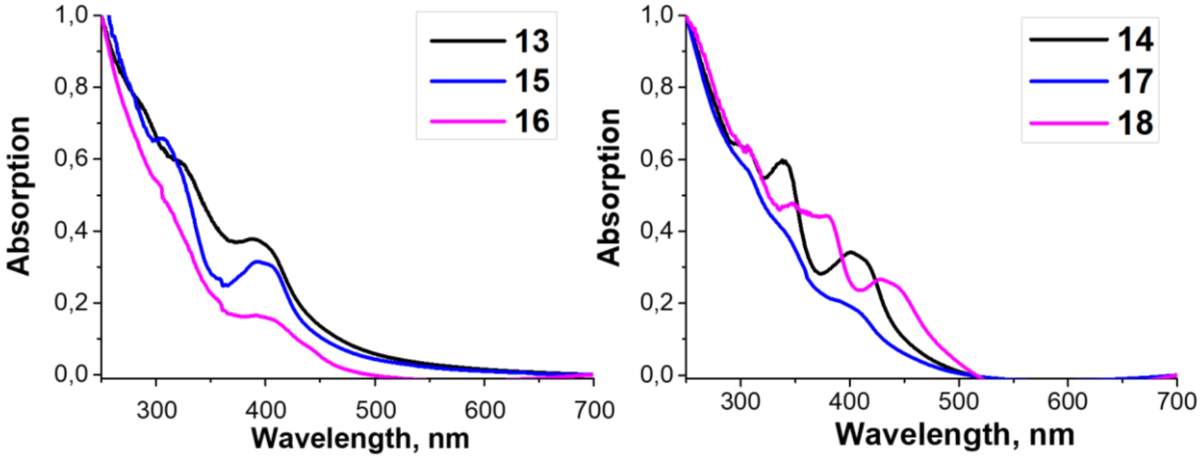

Figure S7. Normalized UV-Vis absorption spectra for **13**–**18** in solid state (KBr) at RT.

Table S4. UV-Vis absorption data for **7**–**18**.

	Absorption: λ_{max}, nm	
Complex	in CH_2Cl_2	in KBr (pellets)
7	277sh (3.20), 348 (0.95), 382sh (0.78)	281sh, 391
8	303 (2.36), 323sh (1.20) 387 (0.71) 404 (0.55)	308, 401
9	283sh (2.89), 378sh (0.60)	304, 399
10	281 (3.59), 402 (1.13)	289sh, 318, 410
11	303 (2.53), 321sh (1.62), 398 (0.66)	307, 401
12	311 (2.49), 338sh (1.15), 414 (1.06)	308sh, 339sh, 422
13	281sh, 314sh, 377	285sh, 324, 389
14	304, 332, 395	304, 339, 403
15	272sh, 305, 380	308, 394
16	280sh, 313sh, 481	310sh, 400
17	264sh, 302, 403sh	305sh, 338sh, 395
18	306sh, 351, 415	307sh, 379, 431

S3. Theoretical studies of chloride complexes

*S3.1. Geometry optimization of complexes **7**, **8**, **11** and **12***

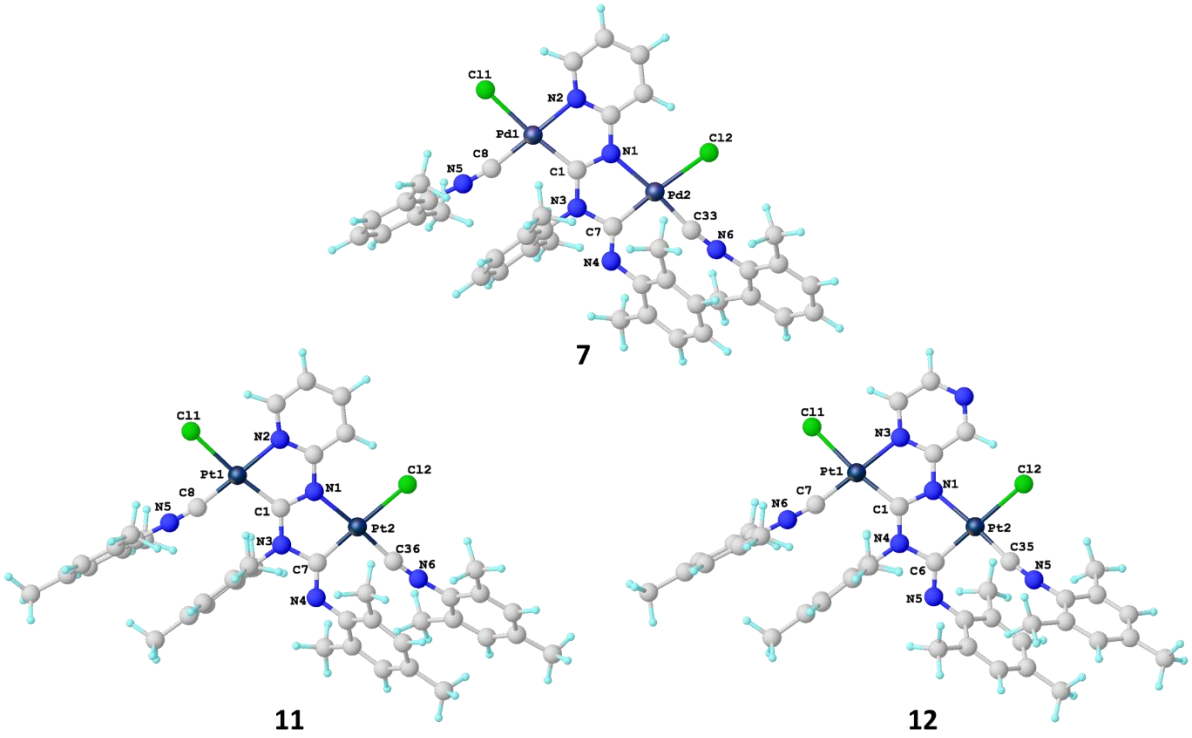

Figure S8. View of optimized structures of complexes **7**, **11** and **12** with the selected atomic numbering schemes. The atomic numbers in complex **8** is analogous to that in **7**.

Table S5. Selected experimental and optimized bond lengths and angles for complexes **7, 8, 11** and **12**

Complex		Experimental values	Optimized values
7	Bonds, Å		
	Pd1–Cl1	2.3469(5)	2.3430
	Pd2–Cl2	2.4082(6)	2.3980
	Pd1–N2	2.0281(17	2.0327
	Pd2–N1	2.0536(17)	2.0836
	Pd1–C8	1.940(2)	1.9157
	Pd2–C33	1.945(2)	1.9169
	Pd1–C1	1.988(2)	1.9912
	Pd2–C7	1.977(2)	1.9785
	C8–N5	1.259(3)	1.1656
	C33–N6	1.153(3)	1.1671
	C1–N1	1.342(3)	1.3352
	C1–N3	1.343(3)	1.3446
	C7–N3	1.458(3)	1.4341
	C7–N4	1.259(3)	1.2663

	Angles, º		
	N2–Pd1–Cl1	100.54(8)	95.656
	C1–Pd1–N2	79.36(8)	78.445
	C8–Pd1–Cl1	86.26(6)	83.619
	C8–Pd1–C1	93.97(5)	102.461
	N1–Pd2–Cl2	96.08(9)	95.656
	C15–Pd2–N1	78.90(8)	79.214
	C33–Pd2–Cl2	83.44(7)	80.701
	C33–Pd2–C7	101.47(5)	96.286
	N5–C8–Pd1	169.25(18)	169.901
	N6–C36–Pd2	171.1(2)	171.321
	C8–N5–C9	175.9(2)	172.830
	C33–N6–C34	172.0(2)	170.870
	N1–C1–N3	116.09(17)	115.286
	N3–C7–N4	114.43(18)	115.351
8	Bonds, Å		
	Pt1–Cl1	2.3549(14)	2.3487
	Pt2–Cl2	2.4083(13)	2.3989
	Pt1–N2	2.030(4)	2.0402
	Pt2–N1	2.059(4)	2.0772
	Pt1–C8	1.913(6	1.8884
	Pt2–C33	1.912(6)	1.8802
	Pt1–C1	1.974(5)	1.9764
	Pt2–C7	1.974(6)	1.9710
	C8–N5	1.158(7)	1.1714
	C33–N6	1.157(7)	1.1729
	C1–N1	1.353(6)	1.3689
	C1–N3	1.349(6)	1.3683
	C7–N3	1.463(7)	1.3674
	C7–N4	1.266(6)	1.3396
	Angles, º		
	N2–Pt1–Cl1	93.80(13)	94.396
	C1–Pt1–N2	79.0(2)	78.404
	C8–Pt1–Cl1	85.40(17)	84.738
	C8–Pt1–C1	101.8(2)	102.510
	N1–Pt2–Cl2	100.57(12)	102.182
	C15–Pt2–N1	79.0(2)	79.134
	C33–Pt2–Cl2	83.28(17)	81.615
	C33–Pt2–C7	97.1(2)	97.113
	N5–C8–Pt1	170.5(5)	170.836
	N6–C33–Pt2	174.3(5)	172.984
	C8–N5–C9	172.2(6)	175.824
	C33–N6–C34	174.5(5)	172.396
	N1–C1–N3	113.3(5)	114.380
	N3–C7–N4	113.1(5)	114.318
11	Bonds, Å		
	Pt1–Cl1	2.3499(16)	2.3514
	Pt2–Cl2	2.3909(16)	2.4012
	Pt1–N2	2.037(4)	2.0399
	Pt2–N1	2.055(4)	2.0777
	Pt1–C8	1.925(6)	1.8893
	Pt2–C36	1.911(7)	1.8817
	Pt1–C1	1.984(6)	1.9743

	Pt2–C7	1.986(5)	1.9716
	C8–N5	1.268(7)	1.1676
	C36–N6	1.398(8)	1.1696
	C1–N1	1.397(7)	1.3508
	C1–N3	1.341(7)	1.3414
	C7–N3	1.450(7)	1.4397
	C7–N4	1.268(7)	1.2704
	Angles, º		
	N2–Pt1–Cl1	94.51(14)	94.673
	C1–Pt1–N2	78.8(2)	78.382
	C8–Pt1–Cl1	84.36(19)	84.551
	C8–Pt1–C1	102.5(2)	102.474
	N1–Pt2–Cl2	101.57(13)	102.212
	C15–Pt2–N1	79.4(2)	79.150
	C36–Pt2–Cl2	81.0(2)	81.399
	C36–Pt2–C7	98.0(3)	97.283
	N5–C8–Pt1	168.6(6)	170.144
	N6–C36–Pt2	170.0(6)	172.027
	C8–N5–C9	179.3(7)	173.593
	C36–N6–C37	178.2(8)	172.027
	N1–C1–N3	114.0(5)	114.510
	N3–C7–N4	113.5(5)	114.390
12	Bonds, Å		
	Pt1–Cl1		2.3453
	Pt2–Cl2		2.3892
	Pt1–N3		2.0381
	Pt2–N1		2.0749
	Pt1–C7		1.8911
	Pt2–C35		1.8808
	Pt1–C1		1.9764
	Pt2–C6		1.9719
	C7–N6		1.1669
	C35–N7		1.1693
	C1–N1		1.3555
	C1–N4		1.3384
	C6–N4		1.4439
	C6–N5		1.2700
	Angles, º		
	N3–Pt1–Cl1		94.030
	C1–Pt1–N3		78.431
	C7–Pt1–Cl1		85.348
	C7–Pt1–C1		102.253
	N1–Pt2–Cl2		101.147
	C6–Pt2–N1		79.130
	C35–Pt2–Cl2		82.345
	C35–Pt2–C6		97.371
	N5–C7–Pt1		170.482
	N6–C35–Pt2		172.145
	C7–N6–C8		175.085
	C35–N7–C36		170.245
	N1–C1–N4		114.329
	N4–C6–N5		114.241

S3.2. TD-DFT calculations

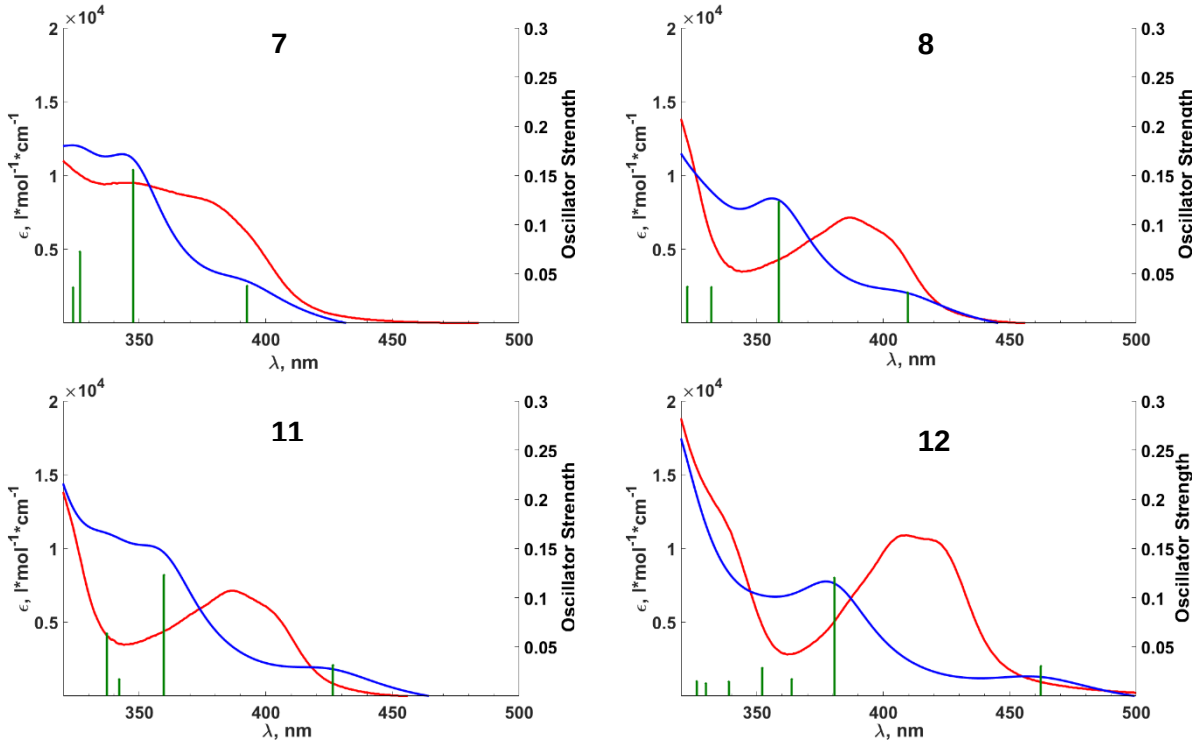

Figure S9. Experimental (red line) and the TD-DFT calculated absorption (blue line) spectra for **7**, **8**, **11** and **12**) in CH_2Cl_2: excitation energies and oscillator strengths are shown by the vertical green bars; the spectrum is convoluted with a Lorenzian function having a full width at half-maximum of 0.35 cm^{-1}. Absorption spectra were calculated from fully optimized geometry in PBE0-D3BJ def2-ZORA-TZVP(–f) in gas phase and using the CPCM model.

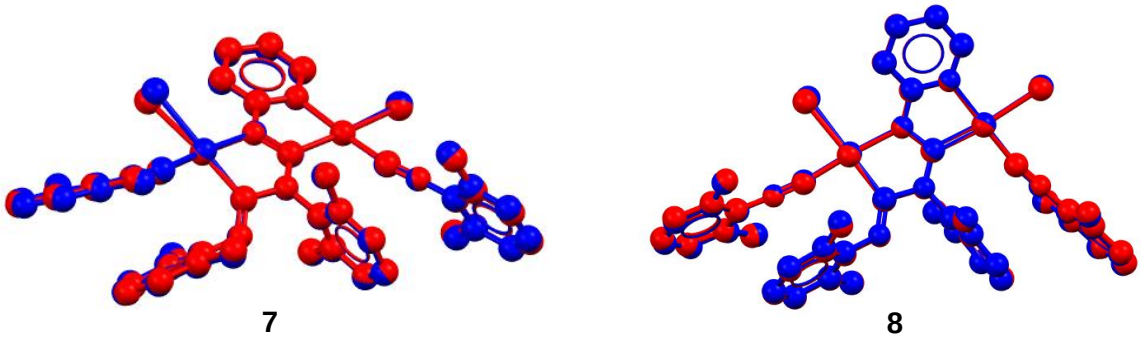

Figure S10. The overlaid geometries optimized in gas phase (red) and in solution (CH_2Cl_2, blue) of **7** and **8**.

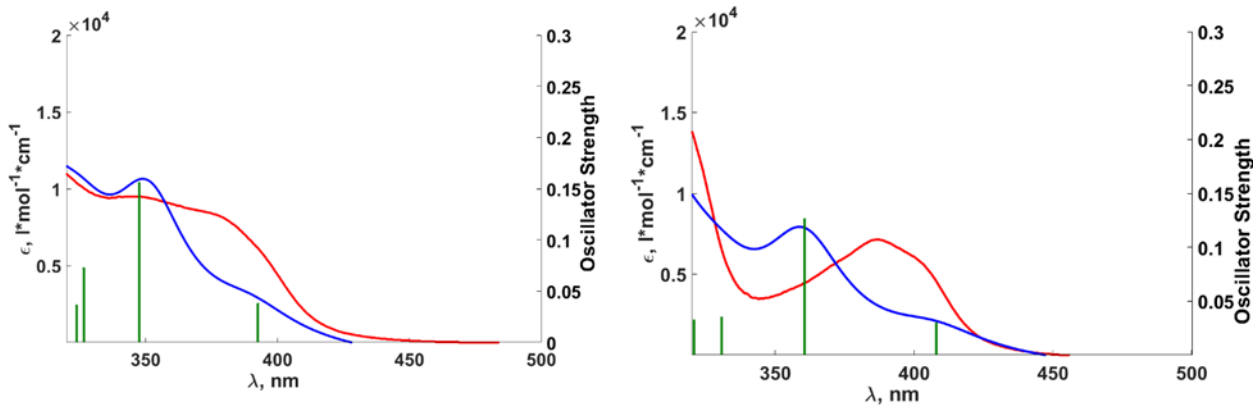

Figure S11. Experimental (red line) and the TD-DFT calculated absorption (blue line) spectra for **7** and **8**) in CH_2Cl_2: excitation energies and oscillator strengths are shown by the vertical green bars; the spectrum is convoluted with a Lorenzian function having a full width at half-maximum of 0.35 cm^{-1}. Absorption spectra were calculated from fully optimized geometry in PBE0-D3BJ def2-ZORA-TZVP(–f) in solution and using the CPCM model.

Table S6. TD-DFT transition energies to the low-lying singlet states with significant oscillator strengths *f*, the main configurations and the characters of the complexes **7**, **8**, **11**, and **12**. Absorption spectra were calculated from fully optimized geometry in PBE0-D3BJ def2-ZORA-TZVP(–f) in gas and using the CPCM model.

	7				**8**			
State	Energy, eV	λ, nm	*f*	Transitions	Energy, eV	λ, nm	*f*	Transitions
S1	3.06	393	0.038	H → L (91%) H → L+5 (2%)	2.93	410	0.031	H → L (92%) H → L+1 (3%)
S2	3.45	348	0.156	H–1 → L (91%) H → L+5 (2%)	3.35	359	0.123	H–1 → L (94%) H → L+1 (3%)
S3	3.67	327	0.072	H–1 → L (3%) H → L+1 (57%) H → L+2 (7%) H → L+3 (15%) H → L+4 (8%)	3.61	332	0.036	H–3 → L (2%) H → L (4%) H → L+1 (68%) H → L+2 (21%)
S4	3.70	324	0.036	H → L (3%) H → L+2 (46%) H → L+3 (31%) H → L+4 (9%) H → L+4 (8%)	3.72	322	0.037	H–3 → L (90%) H → L (4%) H → L+1 (68%) H → L+2 (21%)
S5	3.89	308	0.020	H–3 → L (76%) H–2 → L (8%) H → L+3 (3%) H → L+4 (9%) H → L+4 (8%)	3.83	313	0.018	H–7 → L (2%) H–3 → L (2%) H–2 → L (88%) H–2 → L+1 (3%)
S6	3.92	306	0.035	H–12 → L+1 (3%) H–12 → L+2 (2%) H–1 → L+1 (38%) H–1 → L+2 (24%) H → L+2 (2%)	3.92	306	0.031	H–7 → L (3%) H–4 → L (6%) H → L+1 (5%) H → L+2 (35%)

				H → L+3 (3%)				H → L+3 (26%)
				H → L+4 (7%)				H → L+4 (18%)
S7	3.96	303	0.016	H–1 → L+1 (5%)	3.93	306	0.021	H–4 → L (87%)
				H–1 → L+2 (4%)				H → L+2 (3%)
				H → L+1 (30%)				H → L+1 (5%)
				H → L+3 (34%)				H → L+2 (35%)
				H → L+4 (11%)				H → L+3 (26%)
				H → L+5 (3%)				H → L+4 (18%)
				H → L+4 (7%)				

	11				**12**			
State	Energy, eV	λ, nm	f	Transitions	Energy, eV	λ, nm	f	Transitions
S1	2.81	427	0.031	H → L (93%)	2.60	462	0.030	H → L (95%)
				H → L+1 (3%)				H → L+1 (3%);
S2	3.33	360	0.123	H–2 → L (20%)	3.15	381	0.120	H–3 → L (33%)
				H–1 → L (75%);				H–1 → L (58%);
S3	3.51	342	0.017	H–2 → L (13%)	3.30	364	0.017	H–3 → L (51%)
				H–1 → L (7%)				H–2 → L (5%)
				H → L (3%)				H–1 → L (37%);
				H → L+1 (64%)				
				H → L+2 (9%);				
S4	3.56	337	0.064	H–2 → L (61%)	3.41	352	0.028	H → L (3%)
				H–1 → L (15%)				H → L+1 (86%)
				H → L+1 (16%)				H → L+3 (4%)
				H → L+2 (3%)				H → L+4 (3%);
				H → L+2 (9%);				
S5	3.81	315	0.019	H–3 → L (90%)	3.54	339	0.015	H–7 → L (2%)
				H–3 → L+1 (3%)				H–3 → L (7%)
				H → L+1 (16%)				H–2 → L (85%)
				H → L+2 (3%)				H → L+4 (3%);
				H → L+2 (9%);				
S6	3.84	313	0.065	H → L+2 (26%)	3.64	330	0.013	H–7 → L (6%)
				H → L+3 (33%)				H–5 → L (81%)
				H → L+4 (34%)				H–4 → L (7%)
				H → L+2 (3%)				H → L+4 (3%);
				H → L+2 (9%);				
S7	3.89	308	0.015	H–5 → L (92%)	3.68	326	0.015	H–11 → L (2%)
				H → L+3 (33%)				H–7 → L (46%)
				H → L+4 (34%)				H–6 → L (8%)
				H → L+2 (3%)				H–5 → L (15%)
				H → L+2 (9%);				H–4 → L (15%)
								H–2 → L (5%);

Table S7. TD-DFT transition energies to the low-lying singlet states with significant oscillator strengths *f*, the main configurations and the characters of the complexes **7** and **8**. Absorption spectra were calculated from fully optimized geometry in PBE0-D3BJ def2-ZORA-TZVP(–f) in solution and using the CPCM model.

	7			
State	Energy, eV	λ, nm	f	Transitions
S1	3.08	390	0.038	H → L (91%);
S2	3.42	351	0.162	H–1 → L (92%);
S3	3.68	326	0.056	H–1 → L+1 (2%);
				H → L+1 (54%);
				H → L+2 (21%);

				H → L+3 (5%);
				H → L+5 (8%);
S4	3.73	321	0.037	H–1 → L+1 (2%);
				H → L (3%);
				H → L+2 (4%);
				H → L+3 (73%);
				H → L+5 (8%);
S5	3.87	310	0.048	H–12 → L+1 (2%);
				H–1 → L+1 (45%);
				H–1 → L+2 (17%);
				H–1 → L+3 (8%);
				H → L+2 (3%);
				H → L+5 (4%);
S6	3.89	308	0.008	H–8 → L (3%);
				H–3 → L (71%);
				H–2 → L (11%);
				H–1 → L+3 (8%);
				H → L+2 (3%);
				H → L+5 (4%);
S7	3.94	305	0.021	H–3 → L (4%);
				H → L+1 (35%);
				H → L+2 (21%);
				H → L+3 (13%);
				H → L+5 (17%);
				H → L+5 (4%);
		8		
S1	2.94	408	0.030	H → L (92%);
				H → L+1 (2%);
S2	3.33	360	0.127	H–1 → L (95%);
				H → L+1 (2%);
S3	3.63	331	0.036	H → L (4%);
				H → L+1 (48%);
				H → L+2 (43%);
S4	3.74	321	0.033	H–3 → L (91%);
				H–2 → L (2%);
				H → L+2 (43%);
S5	3.84	313	0.020	H–7 → L (3%);
				H–5 → L (4%);
				H–3 → L (2%);
				H–2 → L (83%);
S6	3.90	308	0.032	H → L (2%);
				H → L+1 (13%);
				H → L+2 (26%);
				H → L+3 (32%);
				H → L+4 (18%);
S7	3.93	305	0.036	H–7 → L (7%);
				H–5 → L (10%);
				H–4 → L (72%);
				H → L+3 (32%);
				H → L+4 (18%);

S3.3. FMO analysis

Table S8. MO contributions of atoms and ligands to FMOs for **7**, **8**, **11** and **12**.

FMO	M, %	Cl, %	CNR, %	Carbene moieties, %	Azaheterocycle fragments, %
			7		
HOMO-1	7	2	3	33	55
HOMO	5	2	10	81	2
LUMO	12	2	11	34	40
LUMO+1	24	3	55	14	8
			8		
HOMO-1	11	4	5	30	50
HOMO	4	2	11	82	1
LUMO	16	3	12	31	38
LUMO+1	10	2	70	13	5
			11		
HOMO-1	7	1	22	43	27
HOMO	3	1	13	82	1
LUMO	16	3	11	30	40
LUMO+1	11	1	64	16	7
			12		
HOMO-1	13	4	8	33	42
HOMO	4	2	11	82	1
LUMO	14	2	8	22	54
LUMO+1	12	2	40	24	22

S3.4 Calculations of one-electron-oxidized forms

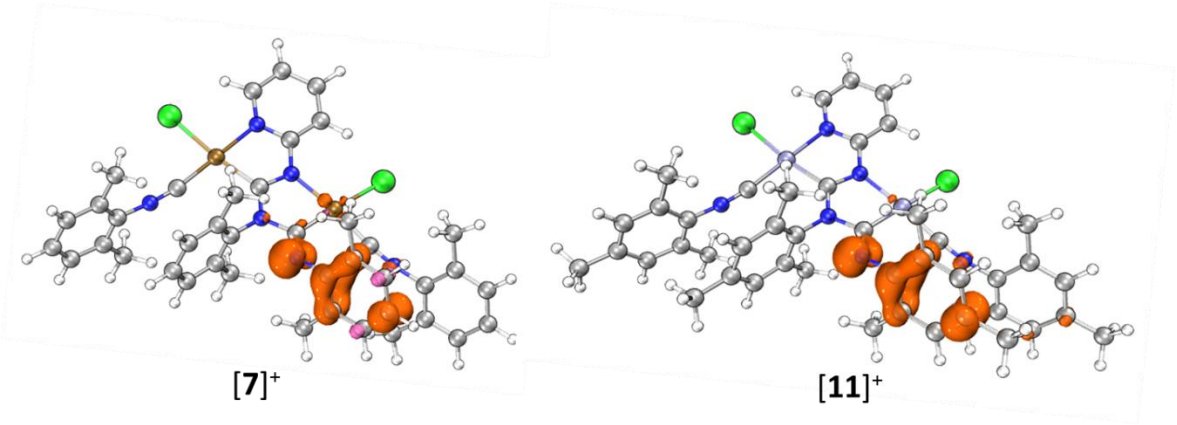

Figure S12. Plots of the spin density calculated for [**7**]$^+$ and [**11**]$^+$.

S3.5. QTAIM and MBO analysis

Table S9. Mayer bond orders and Topological Analysis of Bond Critical Points of complexes **7** and **8**, where G(**r**) – lagrangian kinetic energy, $\nabla^2\rho(\mathbf{r})$ – laplacian of electron density, ELF – electron localization function, MBO – Mayer bond order.

Bond	Optimized bond lengths, Å	MBO	ρ_b	G(r)	V(**r**)	H(**r**)	$\nabla^2\rho(\mathbf{r})$)	ELF	|V(**r**)|/G(**r**)
Pd1–C1	1.9912	0.5512	0.139	0.120	–0.175	–0.056	0.255	0.446	1.47
Pd2–C7	1.9785	0.5491	0.144	0.115	–0.176	–0.061	0.213	0.497	1.54
Pd1–C8	1.9157	0.2675	0.148	0.162	–0.224	–0.061	0.403	0.348	1.38
Pd2–C33	1.9169	0.2753	0.147	0.162	–0.223	–0.061	0.406	0.345	1.38
Pd1–N1	2.0327	0.4195	0.112	0.136	–0.162	–0.026	0.439	0.231	1.19
Pd2–N2	2.0836	0.4360	0.098	0.117	–0.137	–0.020	0.390	0.205	1.17
Pd1–Cl1	2.3430	0.5478	0.079	0.078	–0.097	–0.019	0.234	0.228	1.25
Pd2–Cl2	2.3980	0.6267	0.070	0.069	–0.084	–0.015	0.214	0.198	1.22
N4–C7	1.2663	1.6752	0.392	0.424	–1.117	–0.693	–1.075	0.668	2.63
N3–C7	1.4341	0.9989	0.275	0.132	–0.446	–0.314	–0.731	0.865	3.39
N2–C1	1.3352	1.2570	0.347	0.225	–0.742	–0.517	–1.166	0.827	3.30
N3–C1	1.3446	1.2892	0.335	0.244	–0.761	–0.517	–1.090	0.783	3.12
N2–C2	1.3799	1.0799	0.318	0.151	–0.555	–0.405	–1.015	0.889	3.68
Pt1–C1	1.9764	0.9907	0.161	0.138	–0.225	–0.087	0.204	0.496	1.63
Pt2–C7	1.9710	1.0678	0.165	0.131	–0.223	–0.092	0.156	0.541	1.70
Pt1–C8	1.8884	0.9029	0.176	0.194	–0.295	–0.101	0.373	0.402	1.52
Pt2–C33	1.8802	0.9058	0.179	0.198	–0.302	–0.104	0.379	0.405	1.52
Pt1–N1	2.0402	0.9907	0.125	0.147	–0.193	–0.046	0.407	0.269	1.31
Pt2–N2	2.0772	0.6507	0.113	0.131	–0.169	–0.038	0.371	0.250	1.29
Pt1–Cl1	2.3487	0.6945	0.091	0.083	–0.116	–0.033	0.202	0.286	1.39
Pt2–Cl2	2.3989	0.7788	0.081	0.074	–0.101	–0.027	0.189	0.256	1.36
N4–C7	1.3396	1.6346	0.390	0.402	–1.087	–0.685	–1.135	0.690	2.71
N3–C7	1.3674	0.9715	0.272	0.129	–0.437	–0.308	–0.714	0.865	3.38
N2–C1	1.3689	1.3101	0.337	0.198	–0.673	–0.475	–1.111	0.849	3.41
N3–C1	1.3683	1.2935	0.337	0.244	–0.765	–0.521	–1.109	0.788	3.14
N2–C2	1.3775	1.1067	0.320	0.155	–0.566	–0.411	–1.022	0.884	3.65

S3.6. ETS-NOCV calculations

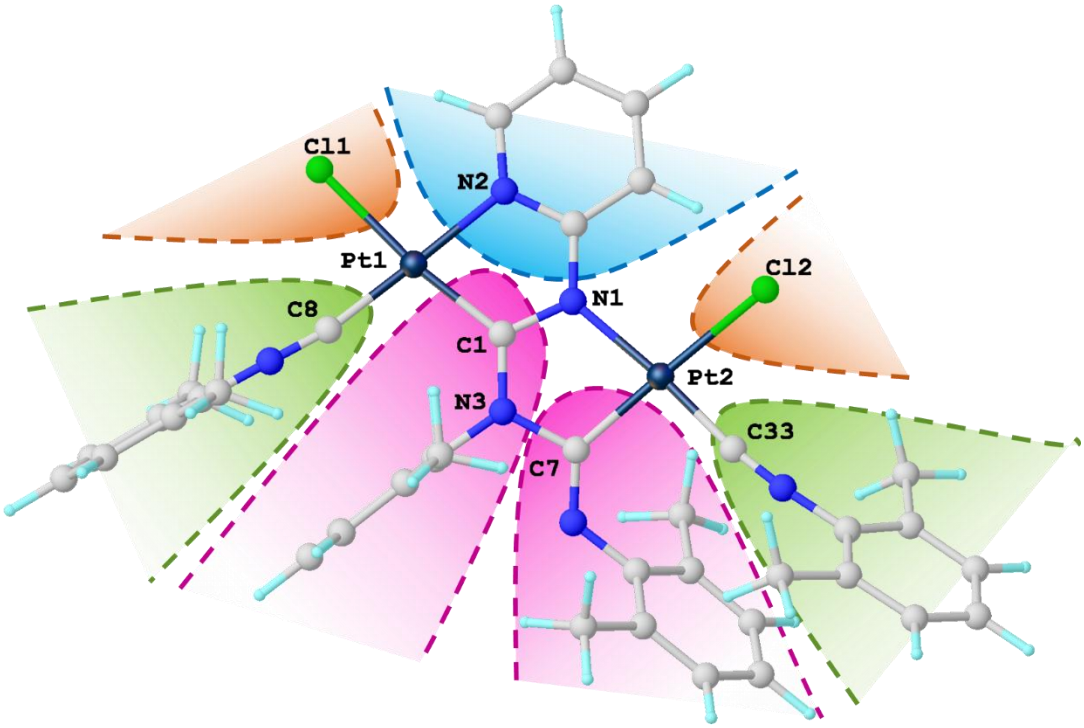

Figure S13. Fragmentation scheme of **8** used for ETS-NOCV analysis.

S4. Theoretical studies of thiocyanate complexes

*S4.1. DFT studies of M–N coordination bonding in structures of **16** and **18***

To establish whether the coordination geometries of the studied compounds, and in particular the bent structure of the fragment M–N=C, are influenced by the crystal packing, quantum chemical calculations were undertaken. We carried out the full geometry optimization procedure for the isolated model species **16** and **18**. If these crystal-packing effects are significant, the structures should change appreciably on going from the solid state to the gas phase, otherwise the geometries are expected to be preserved in the isolated form. We found that both fragments M–N–C in the optimized equilibrium geometries of isolated model species **16** and **18** have a bent structure (**Figure S14**).

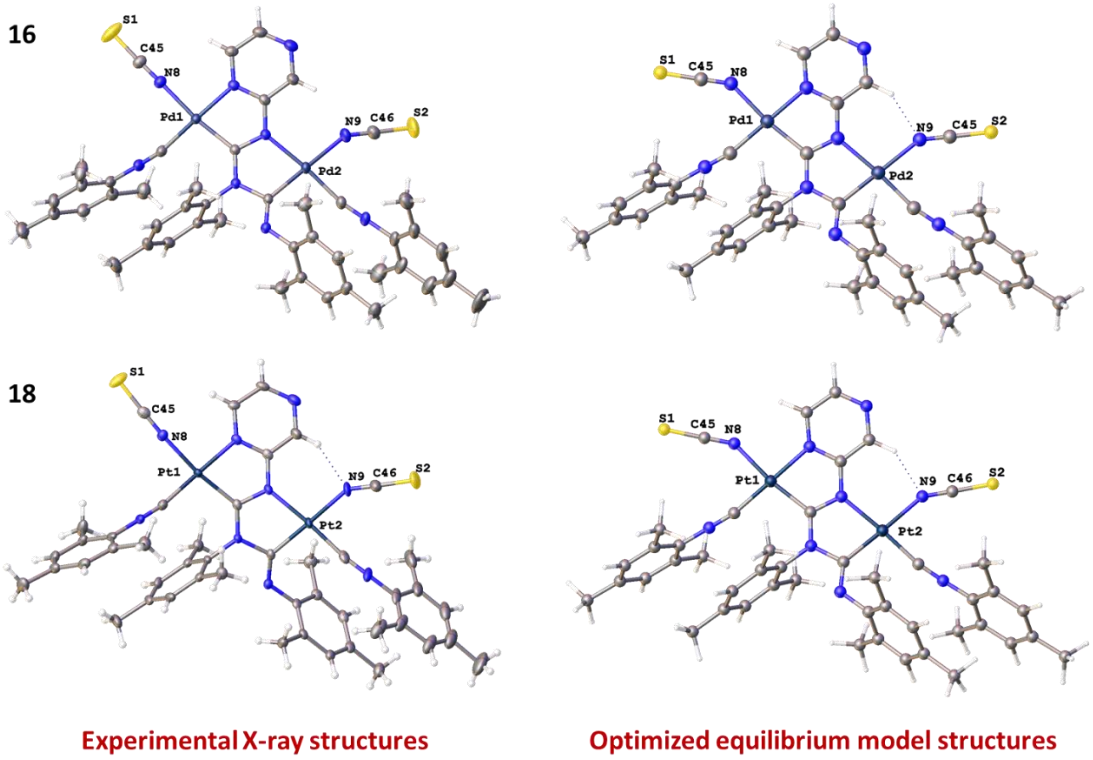

Figure S14. Views of experimentally determined and theoretically calculated structures of **16** and **18**.

Inspection of the data presented in **Table S10** reveals that the geometry optimization procedure affects only marginally the N8(9)–C45(46) and C45(46)–S1(2) bond lengths and the C46–N9–M2 angles, and significantly the M1–N8 bond lengths and the C45–N8–M1 angles.

Table S10. Selected bond lengths and angles for **16**, **18**.

	16		**18**	
	X-ray data	theoretical geometry optimization	X-ray data	theoretical geometry optimization
Bond lengths, Å				
M1–N8	2.031(3)	2.057	2.028(4)	2.063
N8–C45	1.151(4)	1.189	1.154(5)	1.189
C45–S1	1.619(3)	1.612	1.620(4)	1.608
M2–N9	2.096(3)	2.094	2.092(4)	2.094
N9–C46	1.158(5)	1.185	1.161(6)	1.186
C46–S2	1.612(4)	1.618	1.614(5)	1.615
Angles, º				
C45–N8–M1	175.7(3)	142.1	175.6(3)	144.7
C46–N9–M2	147.1(3)	146.5	147.0(4)	148.1

To further rationalize the nature of coordination bonds M–N in **16** and **18**, the QTAIM analysis for the optimized equilibrium geometries of isolated model species was performed (**Table S11**). The values of electron density (0.085–0.106 a.u.), Laplacian of electron density (0.416–0.469 a.u.) and energy density ((–0.026)–(–0.011) a.u.) in the bond critical points (3, –1) corresponding to coordination bonds M–N in the optimized equilibrium geometries of isolated model species **16** and **18** are typical for such closed-shell interactions in similar coordination compounds.[1] The ellipticity of these coordination bonds M–N is low (0.094–0.125) confirming the formal "single" character of these bonds and is well consistent with small values of Wiberg bond indices[2] (0.52–0.42) and Fuzzy bond orders ca. 1[3] (1.03–1.10) for appropriate interatomic contacts.

Table S11. Results of the topological analysis of the electron density distribution and values of the Wiberg bond indices and Fuzzy bond orders corresponding to coordination bonds M–N in the optimized equilibrium geometries of isolated model species **16** and **18**.

	$\rho(\mathbf{r})$, [e/E^3]	$\nabla^2\rho(\mathbf{r})$, [e/E^3]	H_b, [Hartree/E^3]	ε	WI	FBO
	16					
Pd1–N8	0.093	0.441	-0.016	0.125	0.47	1.10
Pd2–N9	0.085	0.416	-0.011	0.115	0.42	1.06
	18					
Pt1–N8	0.106	0.469	-0.026	0.131	0.52	1.08
Pt2–N9	0.097	0.445	-0.021	0.122	0.47	1.03

* $\rho(\mathbf{r})$ – density of all electrons, $\nabla^2\rho(\mathbf{r})$ – Laplacian of electron density, H_b –energy density, ε – ellipticity of electron density, WI – Wiberg bond indices, FBO – Fuzzy bond orders. The Poincare-Hopf relationship (criterion that shows that all critical points were determined) was satisfied in all cases.

The natural bond orbitals (NBO) analysis[4] does not indicate the presence of any σ- or π-type Pd–N and Pt–N bond orbitals for the M–N coordination bonds in the optimized equilibrium model structures **16** and **18**, respectively. This observation may reveal that all Pd–N and Pt–N bond orbitals in the studied systems are totally polarized toward the N atom, and these coordination bonds are almost purely electrostatic. The results of charge decomposition analyses (CDA)[5] calculations reveal that the [M]←L σ-donation totally prevails over the [M]→L π-back-donation for M–N coordination bonds in the optimized equilibrium model structure **16** and **18** (**Table S12**).

Table S12. Results of the charge decomposition analysis (CDA) for M–N coordination bonds in the optimized equilibrium model structures **16** and **18**.

Coordination bond	*d*	*b*	*r*	*N*	E_v
16					
Pd1–N8 2.057 Å	0.244	0.006	–0.219	0.423	136
Pd2–N9 2.094 Å	0.244	0.004	–0.264	0.383	118
18					
Pt1–N8 2.063 Å	0.245	0.005	–0.257	0.421	144
Pt2–N9 2.094 Å	0.247	0.002	–0.307	0.392	125

**d* – [M]←L σ-donation, *b* – [M]→L π-back-donation, *r* – repulsive part, *N* – net electron transfer between the donor and acceptor fragments, E_v, kcal/mol – vertical total energies for M–N coordination bonds cleavage.

The overlap population between the occupied fragment orbitals (FOs) of the two fragments in corresponding complex orbital (term *r*) is negative in both cases. It implies that in this complex orbital, the electrons of occupied FOs are depleted (mainly due to the Pauli repulsion) from the overlap region between the two fragments. The negative values of *r* reveals that repulsive effect dominates the overall interaction between occupied FOs, which results in corresponding electrons moved away toward non-overlapping regions from overlap regions. The amount of net electron transfer between the donor and acceptor fragments was estimated using extended charge decomposition analysis (ECDA) formalism[6]: in both cases the net electron transfer between the donor and acceptor fragments is very similar and quite logical trend is observed – the shorter coordination bond led to higher net electron transfer between the donor and acceptor fragments (**Table S12**). The calculated vertical total energies for M–N coordination bonds cleavage in the optimized equilibrium model structure **16** and **18** are presented in **Table S12**: these contacts in platinum complex are expectedly stronger that those in palladium complex.

*S4.2. DFT studies of noncovalent interactions in structures of **16** and **18***

Table S13. Characteristic parameters of noncovalent contacts in the **16** and **18** structures, where values of the density of all electrons – $\rho(\mathbf{r})$, Laplacian of electron density – $\nabla^2\rho(\mathbf{r})$ and appropriate λ_2 eigenvalues, energy density – H_b, potential energy density – $V(\mathbf{r})$, and Lagrangian kinetic energy – $G(\mathbf{r})$ (a.u.) at the bond critical points (3, –1).

Contact	*d*, Å	$d/\Sigma(R_{vdW})$ (Bondi)	$d/\Sigma(R_{vdW})$ (Alvarez)	$\rho(\mathbf{r})$	$\nabla^2\rho(\mathbf{r})$	λ_2	H_b	$V(\mathbf{r})$	$G(\mathbf{r})$
Pd1•••C5	3.471(13)	1.04	0.89	0.005	0.015	-0.005	0.001	-0.002	0.003
Pt1•••C5	3.479(3)	1.04	0.86	0.008	0.021	-0.008	0.001	-0.004	0.005
16									
N8•••C5	3.392(5)	1.04	0.99	0.005	0.016	-0.005	0.001	-0.003	0.003
S1•••C2	3.618(4)	1.03	0.99	0.006	0.017	-0.006	0.001	-0.002	0.003
18									
S1•••C2	3.570(3)	1.02	0.98	0.006	0.018	-0.006	0.001	-0.003	0.004

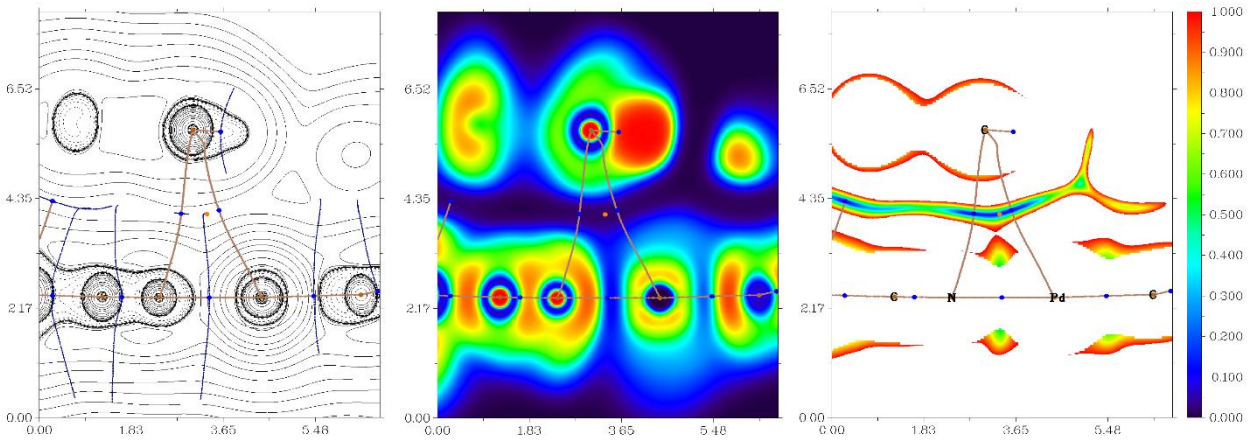

Figure S15. Contour line diagram of the Laplacian of electron density distribution $\nabla^2\rho(\mathbf{r})$, bond paths, and selected zero-flux surfaces (left panel), visualization of electron localization function (ELF, center panel) and reduced density gradient (RDG, right panel) analyses for Pd1•••C5 and N8•••C5 intermolecular contacts in **16**. Bond critical points (3, –1) are shown in blue, nuclear critical points (3, –3) – in pale brown, ring critical points (3, +1) – in orange, bond paths are shown as pale brown lines, length units – Å, and the color scale for the ELF and RDG maps are presented in a.u.

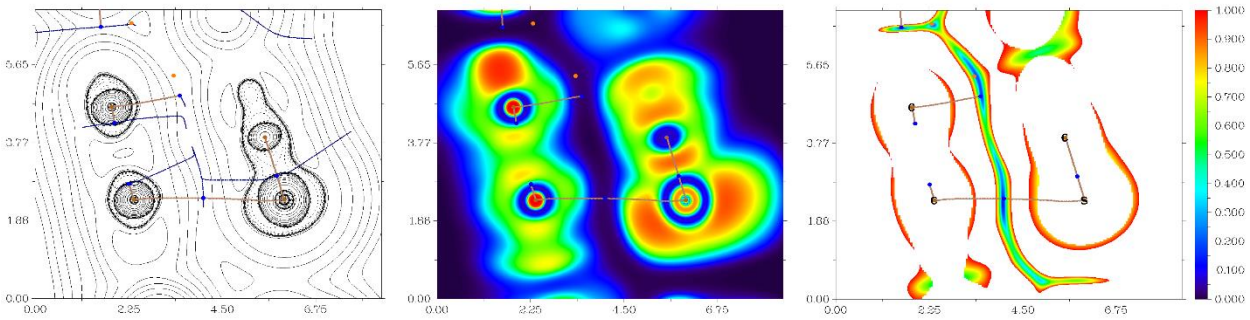

Figure S16. Contour line diagram of the Laplacian of electron density distribution $\nabla^2\rho(\mathbf{r})$, bond paths, and selected zero-flux surfaces (left panel), visualization of electron localization function (ELF, center panel) and reduced density gradient (RDG, right panel) analyses for S1•••C2 intermolecular contacts in **16**. Bond critical points (3, –1) are shown in blue, nuclear critical points (3, –3) – in pale brown, ring critical points (3, +1) – in orange, bond paths are shown as pale brown lines, length units – Å, and the color scale for the ELF and RDG maps are presented in a.u.

Table S14. Cartesian atomic coordinates for model structures.

Atom	X	Y	Z
16 (dimeric supramolecular associate based on the experimental X-ray geometry)			
Pd	14.496848	16.185450	11.586381
Pd	17.053699	20.125209	12.290983
S	11.455291	13.181078	9.446265
S	16.506083	24.491072	10.680384
N	14.584641	17.428510	9.999497
N	16.624919	17.513855	13.286653
N	15.923431	18.624570	11.453353
N	18.539788	18.345963	14.208027
N	13.180987	14.917961	10.681866
N	18.756350	22.341382	13.598657
C	17.594232	18.590865	13.428759
C	15.808433	17.532408	12.225951
C	15.305356	18.542317	10.231277
N	13.843902	14.486601	14.069627
N	14.766583	19.390196	8.066149
C	17.423920	15.286550	13.924185
C	12.461033	14.189441	10.193295
C	19.618103	19.227237	14.451479
C	19.742553	19.759713	15.744701
C	16.672735	16.414581	14.218773
N	16.409470	21.769945	11.148760
C	15.984586	16.556822	15.431215
C	21.795033	20.869500	15.074004
C	14.227544	15.145856	13.210505
C	15.391938	19.509554	9.233013
H	15.907510	20.267790	9.388570

C	20.834404	20.576978	16.018909
H	20.919699	20.938950	16.871657
C	17.399948	14.240772	14.847968
H	17.866958	13.459252	14.656635
C	18.146502	21.447121	13.220695
C	13.373362	13.642124	15.090494
C	13.943287	17.311007	8.829854
H	13.426961	16.556575	8.659530
C	16.699044	14.332301	16.046700
C	20.567132	19.506153	13.468223
C	16.012435	15.499912	16.326095
H	15.558628	15.577556	17.134229
C	12.579013	14.178619	16.093019
C	15.200528	17.808231	15.720615
H	14.494882	17.900162	15.076042
H	14.823306	17.752974	16.601841
H	15.782289	18.569992	15.668887
C	21.648186	20.322182	13.810426
H	22.292810	20.504466	13.166372
C	19.652148	23.364278	13.979027
C	13.287208	11.482848	16.046700
H	13.526949	10.584350	16.045625
C	14.042363	18.286593	7.891805
H	13.582837	18.179387	7.090192
C	12.473203	11.950387	17.054598
C	12.139058	13.299200	17.067567
H	11.601954	13.622334	17.754754
C	13.762132	12.298258	15.035097
C	18.245214	15.193166	12.682099
H	18.893712	15.900938	12.673243
H	18.696007	14.345844	12.659662
H	17.674409	15.272388	11.914411
C	12.189914	15.626691	16.117105
H	11.930226	15.902577	15.234638
H	11.454771	15.750874	16.720750
H	12.937455	16.153755	16.409377
C	20.638503	23.694834	13.060061
C	18.695870	19.480488	16.784096
H	18.550597	18.533659	16.844570
H	18.992470	19.814228	17.633547
H	17.876552	19.915219	16.537142
C	16.456179	22.906016	10.964597
C	11.966324	10.996755	18.110668
H	12.632628	10.328069	18.285512
H	11.781507	11.482198	18.918876
H	11.161948	10.573836	17.801462
C	19.520343	23.928603	15.235194
C	20.444313	18.958526	12.068838
H	19.631016	19.277176	11.670644
H	21.193345	19.250305	11.544138

H	20.430378	17.999020	12.100687
C	20.705404	23.067428	11.692729
H	19.911936	23.288551	11.200712
H	21.475425	23.400179	11.226039
H	20.772332	22.113951	11.781772
C	16.670915	13.179223	17.032365
H	17.028584	13.469827	17.875034
H	15.766002	12.883548	17.154091
H	17.201657	12.454847	16.692922
C	14.644421	11.764855	13.936414
H	15.447048	12.289414	13.888353
H	14.870612	10.850711	14.123968
H	14.178415	11.814361	13.099339
C	22.982360	21.748609	15.396383
H	23.762682	21.202312	15.512755
H	23.127866	22.366923	14.677126
H	22.808791	22.235103	16.206315
C	18.420264	23.531257	16.191215
H	18.297155	22.579944	16.158440
H	18.661508	23.792701	17.082593
H	17.604212	23.968863	15.938610
C	21.481078	25.236909	14.720128
C	21.562036	24.656814	13.480636
H	22.247845	24.909167	12.906560
C	20.468151	24.879761	15.585364
H	20.419055	25.284992	16.421067
C	22.545143	26.268154	15.116618
H	22.155857	27.147171	15.113690
H	22.875080	26.068337	15.994823
H	23.269950	26.239366	14.487367
Pd	15.598753	14.736450	6.941157
Pd	13.041902	10.796691	6.236554
S	18.640310	17.740822	9.081272
S	13.589518	6.430828	7.847153
N	15.510960	13.493390	8.528040
N	13.470682	13.408045	5.240884
N	14.172170	12.297330	7.074184
N	11.555813	12.575937	4.319510
N	16.914614	16.003939	7.845671
N	11.339251	8.580518	4.928881
C	12.501369	12.331035	5.098778
C	14.287168	13.389492	6.301586
C	14.790245	12.379583	8.296261
N	16.251699	16.435299	4.457911
N	15.329018	11.531704	10.461389
C	12.671681	15.635350	4.603352
C	17.634568	16.732459	8.334242
C	10.477498	11.694663	4.076058
C	10.353048	11.162187	2.782836
C	13.422866	14.507319	4.308764

N	13.686131	9.151955	7.378777
C	14.111015	14.365078	3.096322
C	8.300568	10.052400	3.453533
C	15.868057	15.776044	5.317033
C	14.703663	11.412346	9.294524
H	14.188091	10.654110	9.138967
C	9.261197	10.344922	2.508629
H	9.175903	9.982950	1.655880
C	12.695653	16.681128	3.679569
H	12.228643	17.462648	3.870903
C	11.949099	9.474779	5.306843
C	16.722239	17.279776	3.437043
C	16.152314	13.610893	9.697684
H	16.668640	14.365325	9.868007
C	13.396557	16.589599	2.480837
C	9.528469	11.415747	5.059315
C	14.083166	15.421988	2.201442
H	14.536973	15.344344	1.393308
C	17.516588	16.743281	2.434518
C	14.895073	13.113669	2.806922
H	15.600719	13.021738	3.451495
H	15.272295	13.168926	1.925697
H	14.313312	12.351908	2.858651
C	8.447415	10.599718	4.717111
H	7.802791	10.417434	5.361165
C	10.443453	7.557622	4.548510
C	16.808393	19.439052	2.480837
H	16.568652	20.337550	2.481912
C	16.053238	12.635307	10.635733
H	16.512765	12.742513	11.437345
C	17.622398	18.971513	1.472939
C	17.956543	17.622700	1.459970
H	18.493647	17.299566	0.772784
C	16.333469	18.623642	3.492441
C	11.850387	15.728734	5.845438
H	11.201889	15.020962	5.854294
H	11.399594	16.576056	5.867875
H	12.421192	15.649512	6.613127
C	17.905687	15.295209	2.410433
H	18.165375	15.019323	3.292899
H	18.640830	15.171026	1.806787
H	17.158146	14.768145	2.118161
C	9.457098	7.227066	5.467476
C	11.399731	11.441412	1.743441
H	11.545004	12.388241	1.682967
H	11.103131	11.107672	0.893991
H	12.219049	11.006681	1.990395
C	13.639422	8.015884	7.562941
C	18.129277	19.925145	0.416870
H	17.462973	20.593831	0.242025

H	18.314094	19.439702	-0.391339
H	18.933653	20.348064	0.726076
C	10.575259	6.993297	3.292343
C	9.651288	11.963374	6.458699
H	10.464585	11.644724	6.856893
H	8.902256	11.671595	6.983399
H	9.665223	12.922880	6.426851
C	9.390197	7.854472	6.834809
H	10.183665	7.633349	7.326826
H	8.620176	7.521721	7.301499
H	9.323269	8.807949	6.745765
C	13.424686	17.742677	1.495172
H	13.067017	17.452073	0.652503
H	14.329599	18.038352	1.373446
H	12.893944	18.467053	1.834615
C	15.451180	19.157045	4.591124
H	14.648553	18.632486	4.639184
H	15.224989	20.071189	4.403569
H	15.917186	19.107539	5.428198
C	7.113241	9.173291	3.131154
H	6.332919	9.719588	3.014782
H	6.967735	8.554977	3.850411
H	7.286810	8.686797	2.321223
C	11.675337	7.390643	2.336322
H	11.798446	8.341956	2.369098
H	11.434094	7.129199	1.444944
H	12.491390	6.953037	2.588927
C	8.614523	5.684991	3.807409
C	8.533565	6.265086	5.046901
H	7.847756	6.012733	5.620977
C	9.627450	6.042139	2.942173
H	9.676546	5.636908	2.106470
C	7.550458	4.653746	3.410920
H	7.939744	3.774729	3.413847
H	7.220521	4.853563	2.532714
H	6.825651	4.682534	4.040170
18 (dimeric supramolecular associate based on the experimental X-ray geometry)			
Pt	-1.833565	15.875061	11.629371
Pt	0.717147	19.818671	12.312841
S	-4.916942	13.047079	9.283423
S	0.057769	24.150168	10.667987
N	-1.714410	17.109548	10.019025
N	-0.384502	18.311813	11.473531
N	0.310963	17.196792	13.305578
N	-3.168932	14.641790	10.730879
N	-2.439213	14.175171	14.101846
N	2.220691	18.033665	14.228188
N	0.032794	21.418854	11.151833
C	-0.517061	17.215031	12.261265
C	1.275620	18.287798	13.439341

N	2.361264	22.038377	13.645272
N	-1.437202	19.003685	8.035219
C	-0.978648	18.213017	10.240911
C	-0.343461	16.269027	15.455984
C	-2.084705	14.819925	13.235265
C	-3.900837	13.970893	10.142584
C	3.401966	19.451152	15.775085
C	-2.493602	12.019302	15.142449
C	4.121508	18.716722	12.098004
H	4.088601	17.757464	12.118022
H	4.884620	18.999399	11.587387
H	3.321354	19.055940	11.690371
C	-0.305245	15.217235	16.365050
H	-0.757225	15.302929	17.173915
C	0.359119	16.110042	14.253790
C	1.106498	14.975870	13.977360
C	-1.132445	17.518105	15.717572
H	-1.833713	17.596442	15.067275
H	-0.553163	18.281171	15.658001
H	-1.515645	17.475942	16.597604
C	4.233416	19.245658	13.502419
C	3.284342	18.936200	14.481984
C	-0.847090	19.145038	9.209399
H	-0.320964	19.897920	9.354683
C	1.098007	13.946878	14.914255
H	1.580988	13.171561	14.741068
C	0.385906	14.048105	16.103462
C	-2.879714	13.355929	15.157291
C	-2.187565	17.908119	7.866207
H	-2.626601	17.792574	7.054058
C	-4.138155	13.048599	17.138684
H	-4.686334	13.382528	17.811060
C	5.303648	20.078275	13.860480
H	5.939909	20.290093	13.216879
C	-2.338722	16.953907	8.829075
H	-2.864887	16.204156	8.668022
C	4.479099	20.284074	16.077489
H	4.549296	20.639585	16.934701
C	5.448354	20.595659	15.133173
C	-2.955633	11.208876	16.166540
H	-2.701630	10.314519	16.189768
C	1.939429	14.873731	12.721364
H	1.389697	15.060865	11.957358
H	2.298933	13.986913	12.648379
H	2.657927	15.508636	12.762773
C	-3.695855	13.909183	16.146132
C	1.771843	21.155602	13.207436
C	-4.089871	15.359805	16.147988
H	-3.341409	15.894364	16.423713
H	-4.819868	15.492798	16.756172

H	-4.358646	15.618709	15.263169
C	-3.791141	11.704069	17.160947
C	2.344260	19.150206	16.791755
H	1.534546	19.608435	16.556233
H	2.639359	19.444768	17.656333
H	2.182145	18.204232	16.813962
C	-1.589162	11.465136	14.058990
H	-2.060997	11.454861	13.222705
H	-1.325674	10.570992	14.288390
H	-0.808880	12.018390	13.979196
C	6.619541	21.483907	15.474536
H	7.352032	20.943906	15.780335
H	6.363820	22.097563	16.167746
H	6.886871	21.975057	14.695003
C	3.264065	23.034235	14.073832
C	-4.311600	10.769920	18.233275
H	-4.584772	11.281468	18.998189
H	-3.617728	10.157692	18.488722
H	-5.062398	10.278435	17.892115
C	0.360850	12.914541	17.101580
H	0.745024	13.209712	17.930036
H	0.868924	12.175551	16.758379
H	-0.546240	12.638218	17.249127
C	3.129349	23.563779	15.355801
C	2.034030	23.164037	16.270433
H	1.191565	23.437594	15.899404
H	2.159821	23.585362	17.123453
H	2.040613	22.210433	16.379818
C	0.053897	22.563969	10.964454
C	5.194087	24.330127	13.600746
H	5.877296	24.600705	13.029853
C	4.317274	22.791046	11.793745
H	4.405236	21.837868	11.866359
H	5.070673	23.146193	11.315836
H	3.509640	23.002043	11.318470
C	4.263939	23.390811	13.153634
C	4.102375	24.502488	15.726849
H	4.056245	24.887577	16.571408
C	5.120820	24.872135	14.882716
C	6.202315	25.841850	15.352091
H	6.865227	25.363589	15.856159
H	5.806849	26.518948	15.907345
H	6.615448	26.254420	14.590608
Pt	-0.736169	14.523539	6.923004
Pt	-3.286882	10.579929	6.239535
S	2.347207	17.351521	9.268952
S	-2.627503	6.248432	7.884389
N	-0.855325	13.289052	8.533351
N	-2.185232	12.086787	7.078844
N	-2.880697	13.201808	5.246797

N	0.599197	15.756810	7.821496
N	-0.130521	16.223429	4.450529
N	-4.790425	12.364935	4.324188
N	-2.602529	8.979746	7.400543
C	-2.052674	13.183569	6.291111
C	-3.845354	12.110802	5.113035
N	-4.930998	8.360223	4.907103
N	-1.132532	11.394915	10.517156
C	-1.591087	12.185583	8.311464
C	-2.226273	14.129573	3.096391
C	-0.485030	15.578675	5.317111
C	1.331102	16.427707	8.409792
C	-5.971701	10.947448	2.777291
C	-0.076133	18.379298	3.409927
C	-6.691242	11.681878	6.454371
H	-6.658335	12.641136	6.434353
H	-7.454354	11.399201	6.964988
H	-5.891089	11.342660	6.862004
C	-2.264490	15.181365	2.187325
H	-1.812509	15.095671	1.378460
C	-2.928854	14.288558	4.298585
C	-3.676233	15.422730	4.575016
C	-1.437289	12.880495	2.834803
H	-0.736021	12.802158	3.485101
H	-2.016572	12.117429	2.894375
H	-1.054090	12.922658	1.954771
C	-6.803150	11.152942	5.049957
C	-5.854077	11.462400	4.070391
C	-1.722644	11.253562	9.342976
H	-2.248771	10.500680	9.197693
C	-3.667742	16.451722	3.638121
H	-4.150722	17.227039	3.811307
C	-2.955640	16.350495	2.448914
C	0.309980	17.042671	3.395085
C	-0.382170	12.490481	10.686168
H	0.056867	12.606026	11.498317
C	1.568421	17.350001	1.413691
H	2.116599	17.016072	0.741316
C	-7.873382	10.320325	4.691896
H	-8.509644	10.108507	5.335496
C	-0.231013	13.444693	9.723300
H	0.295153	14.194444	9.884353
C	-7.048833	10.114526	2.474887
H	-7.119030	9.759015	1.617674
C	-8.018089	9.802941	3.419203
C	0.385899	19.189724	2.385835
H	0.131895	20.084081	2.362608
C	-4.509164	15.524869	5.831012
H	-3.959432	15.337735	6.595017
H	-4.868667	16.411687	5.903997

H	-5.227662	14.889964	5.789603
C	1.126120	16.489417	2.406243
C	-4.341578	9.242998	5.344939
C	1.520136	15.038795	2.404388
H	0.771675	14.504236	2.128662
H	2.250134	14.905802	1.796204
H	1.788911	14.779891	3.289206
C	1.221406	18.694531	1.391428
C	-4.913995	11.248394	1.760620
H	-4.104281	10.790165	1.996143
H	-5.209094	10.953832	0.896043
H	-4.751879	12.194368	1.738413
C	-0.980573	18.933464	4.493385
H	-0.508738	18.943739	5.329671
H	-1.244061	19.827608	4.263985
H	-1.760854	18.380210	4.573179
C	-9.189275	8.914693	3.077839
H	-9.921767	9.454694	2.772040
H	-8.933555	8.301037	2.384630
H	-9.456606	8.423543	3.857373
C	-5.833800	7.364365	4.478543
C	1.741865	19.628680	0.319101
H	2.015038	19.117132	-0.445814
H	1.047994	20.240908	0.063653
H	2.492664	20.120165	0.660260
C	-2.930584	17.484059	1.450796
H	-3.314759	17.188888	0.622339
H	-3.438658	18.223049	1.793996
H	-2.023494	17.760382	1.303249
C	-5.699084	6.834821	3.196574
C	-4.603765	7.234563	2.281942
H	-3.761300	6.961006	2.652971
H	-4.729556	6.813238	1.428923
H	-4.610347	8.188167	2.172557
C	-2.623632	7.834631	7.587922
C	-7.763821	6.068473	4.951629
H	-8.447030	5.797895	5.522523
C	-6.887009	7.607554	6.758630
H	-6.974970	8.560732	6.686016
H	-7.640407	7.252407	7.236540
H	-6.079374	7.396557	7.233905
C	-6.833673	7.007789	5.398741
C	-6.672109	5.896112	2.825527
H	-6.625980	5.511023	1.980967
C	-7.690554	5.526465	3.669660
C	-8.772050	4.556750	3.200285
H	-9.434961	5.035011	2.696217
H	-8.376583	3.879652	2.645031
H	-9.185182	4.144180	3.961767
16 (optimized equilibrium model structure)			

Pd	-2.808334	1.979825	0.016994
Pd	1.928745	1.170837	-0.158452
S	-7.343744	2.730750	0.320977
S	5.668820	3.841493	-1.130402
N	-1.640252	3.651266	0.109265
N	-0.596194	-0.097435	0.211925
N	0.047608	2.061101	0.002426
N	1.061511	-1.558610	0.791475
N	-4.572557	3.036981	0.060304
N	4.705369	-0.161994	-0.524169
C	0.817148	-0.398025	0.353589
C	-0.964602	1.181671	0.065904
C	-0.321508	3.388958	0.047985
N	-4.777705	-0.380943	-0.358475
N	0.168271	5.721958	0.156138
C	-2.089349	-1.470501	1.577684
C	-5.747632	2.896365	0.170998
C	2.358114	-2.053311	0.992781
C	2.854647	-2.994544	0.080047
C	-1.531014	-1.181908	0.333167
N	3.094258	2.834888	-0.664496
C	-1.811998	-1.940895	-0.806381
C	4.930792	-3.109529	1.348583
C	-3.933253	0.397914	-0.196180
C	0.583100	4.468467	0.074067
H	1.648698	4.278951	0.013568
C	4.137030	-3.502035	0.272932
H	4.532082	-4.217117	-0.446565
C	-2.981648	-2.539669	1.657296
H	-3.434268	-2.775962	2.617771
C	3.614691	0.203571	-0.361771
C	-5.778411	-1.328646	-0.508875
C	-2.068632	4.920480	0.187794
H	-3.142613	5.061550	0.228466
C	-3.304257	-3.311197	0.543367
C	3.113953	-1.670820	2.113454
C	-2.702624	-3.001630	-0.678483
H	-2.946951	-3.597135	-1.555880
C	-5.952108	-1.919991	-1.764951
C	-1.204329	-1.578283	-2.134748
H	-1.575076	-0.606393	-2.484436
H	-1.446246	-2.327564	-2.893404
H	-0.114975	-1.499686	-2.067475
C	4.391138	-2.206873	2.264275
H	4.988957	-1.899709	3.120733
C	6.026514	-0.578272	-0.580483
C	-7.534878	-2.623926	0.438129
H	-8.154969	-2.895864	1.288660
C	-1.150591	5.950650	0.212871
H	-1.476046	6.983363	0.280573

C	-7.740714	-3.254968	-0.788997
C	-6.942227	-2.890849	-1.875417
H	-7.099659	-3.370621	-2.838305
C	-6.558310	-1.647143	0.608648
C	-1.766748	-0.630045	2.782302
H	-0.685490	-0.509528	2.899657
H	-2.164138	-1.084655	3.693496
H	-2.201310	0.373550	2.689419
C	-5.107037	-1.502116	-2.935724
H	-5.253833	-0.440183	-3.163099
H	-5.363478	-2.079149	-3.827451
H	-4.042064	-1.646530	-2.725557
C	6.900387	-0.115619	0.411027
C	2.028373	-3.390819	-1.113920
H	0.990348	-3.589167	-0.826135
H	2.438737	-4.281872	-1.598280
H	2.004666	-2.585313	-1.859753
C	4.184819	3.253845	-0.863862
C	-8.825229	-4.288802	-0.950008
H	-9.031607	-4.800395	-0.005535
H	-8.550873	-5.041607	-1.694829
H	-9.758349	-3.819634	-1.283049
C	6.416969	-1.443323	-1.607264
C	2.566020	-0.689127	3.115546
H	2.439073	0.307796	2.676576
H	3.236449	-0.595649	3.974633
H	1.583110	-1.007660	3.480950
C	6.422823	0.834469	1.471642
H	6.150968	1.799525	1.026219
H	7.202731	1.009143	2.216928
H	5.536988	0.439471	1.981697
C	-4.284565	-4.450761	0.638956
H	-3.775582	-5.415905	0.535311
H	-5.036154	-4.384554	-0.154932
H	-4.808688	-4.447168	1.598627
C	-6.340856	-0.947561	1.919738
H	-5.304337	-1.061648	2.257481
H	-7.002655	-1.350527	2.689983
H	-6.543496	0.125902	1.820037
C	6.327370	-3.647238	1.524035
H	6.356325	-4.445783	2.275006
H	7.012971	-2.858386	1.849834
H	6.715501	-4.053444	0.585231
C	5.432670	-1.881905	-2.654812
H	4.566095	-2.369317	-2.195710
H	5.893617	-2.583458	-3.354606
H	5.061477	-1.023486	-3.226129
C	8.652573	-1.441717	-0.642037
C	8.214828	-0.569341	0.354903
H	8.917889	-0.226938	1.110310

C	7.741785	-1.867456	-1.610145
H	8.072899	-2.545162	-2.393442
C	10.090515	-1.889856	-0.691529
H	10.694716	-1.186553	-1.276660
H	10.186569	-2.874089	-1.159711
H	10.527256	-1.944410	0.310118
18 (optimized equilibrium model structure)			
Pt	-2.773820	1.743133	0.022805
Pt	1.969938	1.001800	-0.148366
S	-7.321558	2.621524	0.355972
S	5.562971	3.884706	-1.153724
N	-1.624651	3.436976	0.127454
N	-0.543290	-0.292008	0.246735
N	0.082718	1.872596	0.032406
N	1.123337	-1.742200	0.812041
N	-4.547526	2.795831	0.044001
N	4.739600	-0.272864	-0.530023
C	0.878386	-0.575598	0.379260
C	-0.932567	0.976646	0.092466
C	-0.299997	3.193428	0.087811
N	-4.701239	-0.622371	-0.349380
N	0.149868	5.533377	0.238998
C	-2.017677	-1.721538	1.574368
C	-5.725612	2.709117	0.177022
C	2.431826	-2.214493	0.999402
C	2.943178	-3.128994	0.068420
C	-1.460400	-1.392418	0.340157
N	3.069460	2.700075	-0.686654
C	-1.724439	-2.123929	-0.820639
C	5.021575	-3.239026	1.333287
C	-3.874957	0.175567	-0.180411
C	0.585222	4.289407	0.150947
H	1.654399	4.119287	0.116545
C	4.232324	-3.623488	0.251935
H	4.635831	-4.321616	-0.479490
C	-2.889779	-2.809066	1.622322
H	-3.341368	-3.078952	2.574409
C	3.653152	0.102903	-0.354957
C	-5.688732	-1.581602	-0.501713
C	-2.074852	4.701490	0.211701
H	-3.151028	4.826815	0.233974
C	-3.191652	-3.558855	0.487817
C	3.184882	-1.840196	2.124931
C	-2.592864	-3.205936	-0.723746
H	-2.821155	-3.784210	-1.616820
C	-5.862360	-2.166527	-1.760766
C	-1.123579	-1.706183	-2.135849
H	-1.524394	-0.736808	-2.458754
H	-1.339035	-2.441168	-2.916190
H	-0.037541	-1.593743	-2.061600

C	4.470751	-2.358218	2.263760
H	5.065345	-2.056859	3.124687
C	6.066493	-0.668342	-0.567454
C	-7.428353	-2.900153	0.445163
H	-8.042262	-3.183200	1.296576
C	-1.174437	5.742678	0.266554
H	-1.516766	6.769394	0.338549
C	-7.632838	-3.525859	-0.785020
C	-6.843300	-3.146505	-1.872938
H	-7.000417	-3.621956	-2.838052
C	-6.461358	-1.914115	0.616549
C	-1.711698	-0.905614	2.799697
H	-0.632266	-0.775823	2.923460
H	-2.107271	-1.385888	3.698421
H	-2.157385	0.094500	2.726403
C	-5.025699	-1.731307	-2.931228
H	-5.184494	-0.669427	-3.150843
H	-5.278023	-2.304914	-3.826357
H	-3.958738	-1.865028	-2.724280
C	6.919873	-0.182105	0.430554
C	2.122535	-3.510675	-1.134230
H	1.086350	-3.725254	-0.851498
H	2.542985	-4.387236	-1.636271
H	2.090330	-2.690061	-1.863267
C	4.129750	3.191021	-0.886956
C	-8.707312	-4.569834	-0.948257
H	-8.914029	-5.080396	-0.003339
H	-8.422110	-5.322502	-1.689185
H	-9.642813	-4.110323	-1.288060
C	6.487132	-1.529845	-1.584957
C	2.623011	-0.887633	3.147493
H	2.487121	0.117307	2.730582
H	3.288715	-0.808172	4.011762
H	1.641960	-1.225343	3.500440
C	6.407521	0.764280	1.478571
H	6.099228	1.713515	1.023109
H	7.179548	0.977442	2.221871
H	5.536294	0.343022	1.993198
C	-4.149140	-4.719894	0.550048
H	-3.623701	-5.670797	0.405467
H	-4.910051	-4.638275	-0.233584
H	-4.663460	-4.762320	1.514080
C	-6.245435	-1.215969	1.928947
H	-5.207275	-1.323852	2.263755
H	-6.902571	-1.624396	2.700276
H	-6.454391	-0.143377	1.833657
C	6.425937	-3.759530	1.499214
H	6.474610	-4.541608	2.266294
H	7.108051	-2.956782	1.797864
H	6.804563	-4.181259	0.563429

C	5.525381	-1.987574	-2.645190
H	4.652914	-2.474329	-2.197333
H	6.003862	-2.694282	-3.327868
H	5.160337	-1.138023	-3.233606
C	8.710325	-1.479828	-0.592164
C	8.243862	-0.609002	0.393349
H	8.931020	-0.247861	1.154701
C	7.819718	-1.928663	-1.568667
H	8.173351	-2.604467	-2.343777
C	10.156849	-1.901544	-0.620970
H	10.754620	-1.194318	-1.208014
H	10.275834	-2.889336	-1.076255
H	10.583647	-1.936360	0.385825

S5. CCDC search

This search was conducted using the ConQuest program (v 2.0.1) for crystal structures of Pd^{II} and Pt^{II} complexes with monodentate N-coordinated thiocyanates ligands with the following secondary search criteria: atomic coordinates error free after CSD checks; no disorder in the crystal structure; no powder studies, and a crystallographic R factor < 0.1. The processing of the CSD data revealed 52 structures with palladium (31 examples) and platinum (21 examples) metal centres. The coordination angle ∠M–N=C in obtained entries varies in the 155.747–180.0° range, while the values of M–N bond length slightly change in the range of 0,16 Å (from 1.969 to 2.13 Å and 1.958 to 2.113 Å for Pd–N and Pt–N bonds respectively), but generally one can notice the tendency of M–N distance's decreasing with M–N=C angle's growth (**Figure S17**). The average values of N–C and C–S bonds in isothiocyanate ligand are also vary in 3σ range (1.141 ± 0.017 Å and 1.623 ± 0.014 Å for palladium complexes: 1.138 ± 0.020 Å and 1.623 ± 0.012 Å for platinum respectively) and are close to meanings for a triple C≡N bond[7] and a double C=S bond[7].

Thus, the large variety of ∠M–N=C angle together with insignificant changes in the structure of the N=C=S fragment is most likely associated with packing effects that is in agreement with reports in previous works[8].

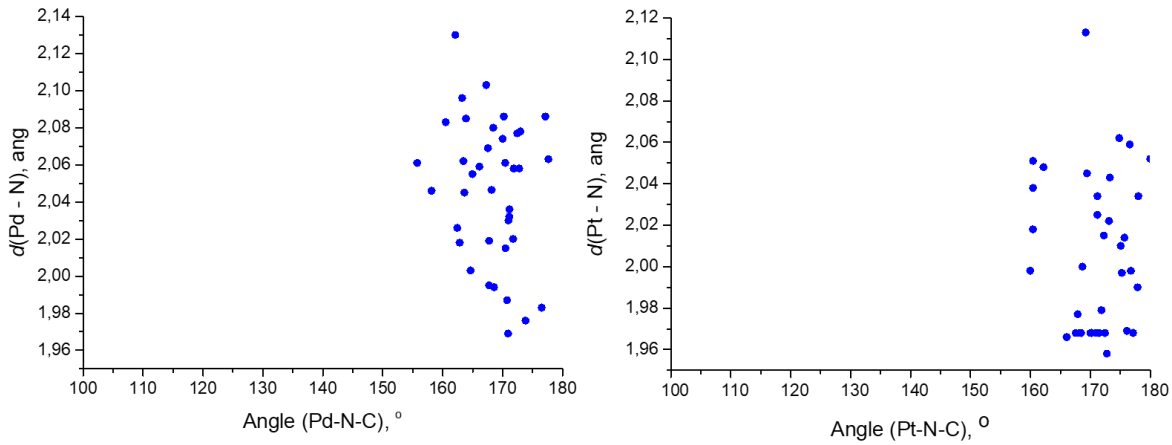

Figure S17. The dependence *d*(M–N)/∠(M–N=C) (M = Pd (left), Pt (right)) according to the CSD search.

S6. Hirshfeld analysis

Table S15. Results of the Hirshfeld surface analysis.

X-ray structure	Contributions of different intermolecular contacts to the molecular Hirshfeld surface*
16	H–H 51.7%, C–H 8.9%, S–H 9.5%, N–H 4.9%, Pd–H 1.1%, C–C 1.0%, S–C 0.7%, C–N 0.6%, C–S 0.6%, N–S 0.4%, N–N 0.3%.
18	H–H 51.0%, C–H 9.2%, S–H 9.1%, N–H 5.1%, C–C 1.2%, Pt–H 1.1%, S–C 0.7%, C–N 0.6%, C–S 0.6%, N–S 0.4%, N–N 0.3%,C–Pt 0.1%.

*The contributions of all other intermolecular contacts do not exceed 0%.

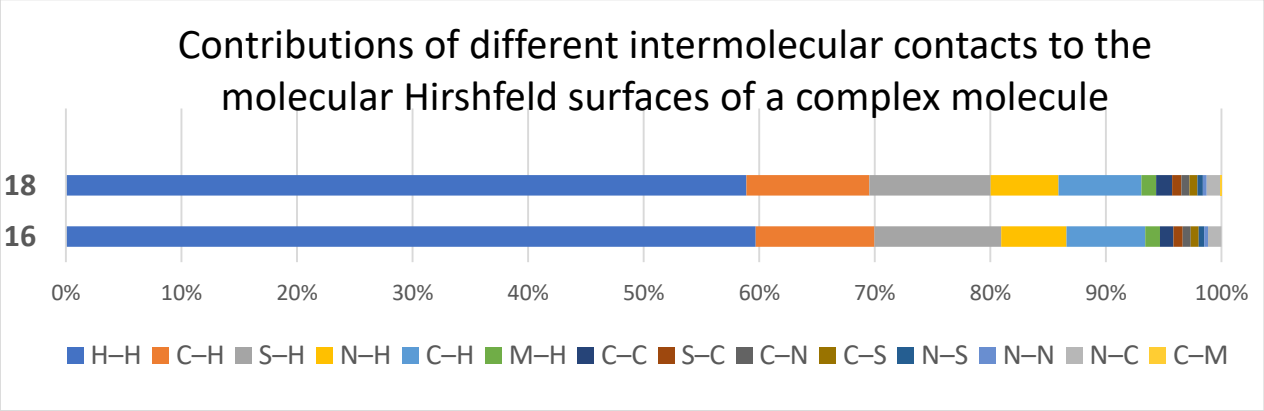

Figure S18. Contributions of various intermolecular contacts to the molecular Hirshfeld surfaces of **16** and **18** complex molecules.

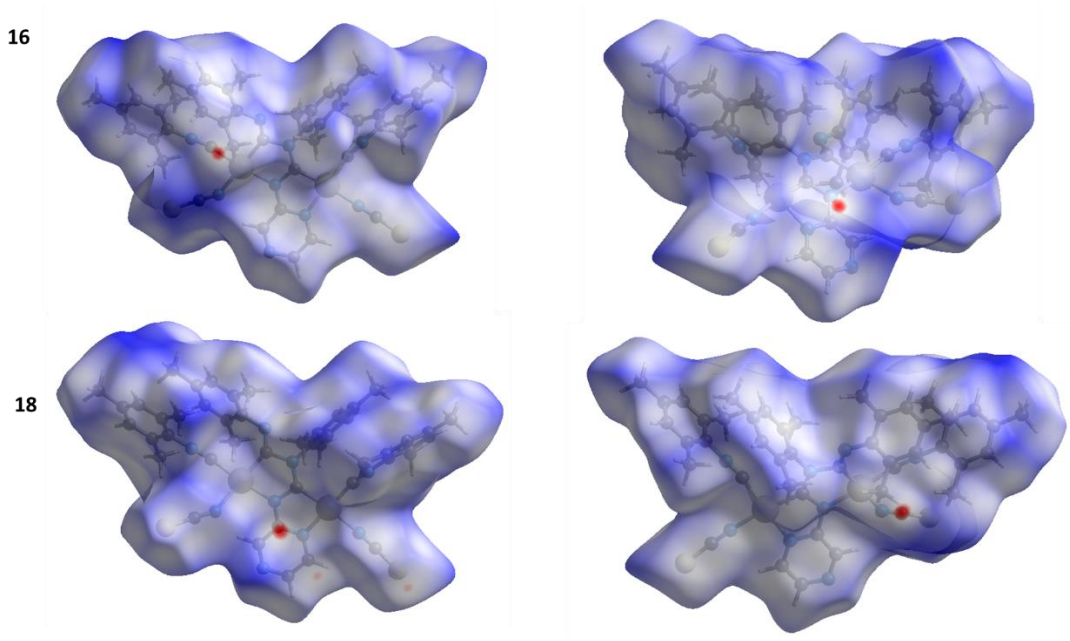

Figure S19. Hirshfeld surfaces for **16** and **18**.

S7. NMR spectra for complexes **9**–**18**

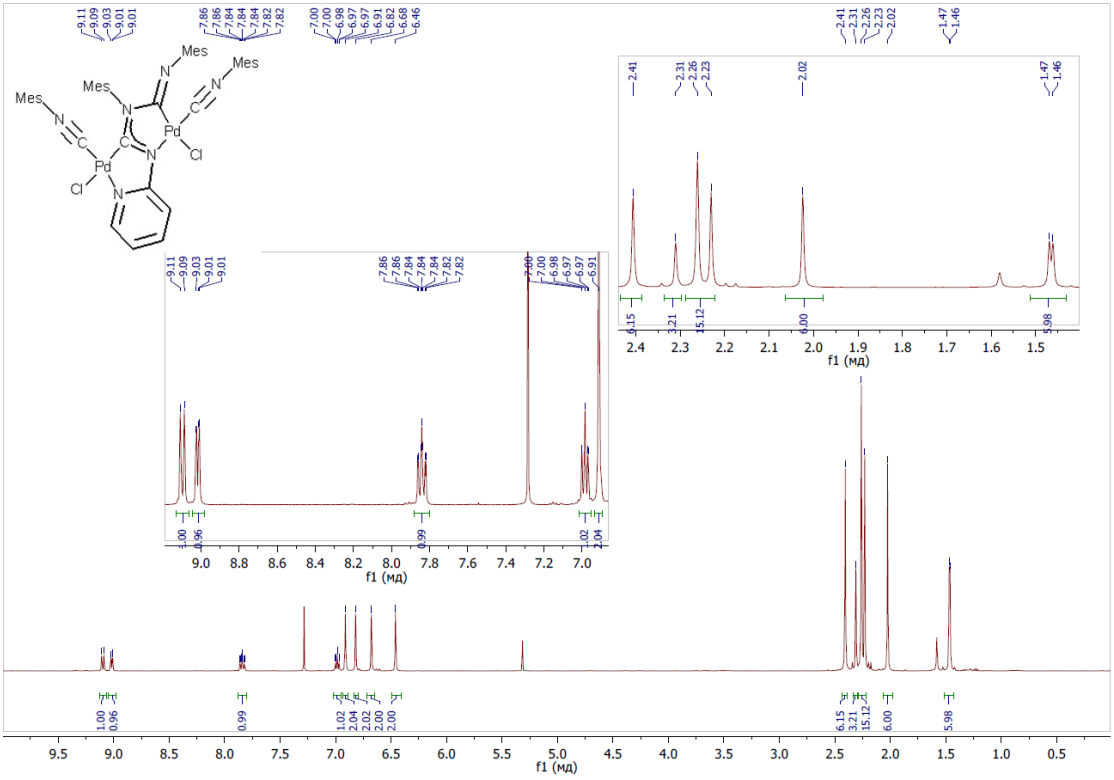

Figure S20. The ^{1}H NMR spectra of **9**.

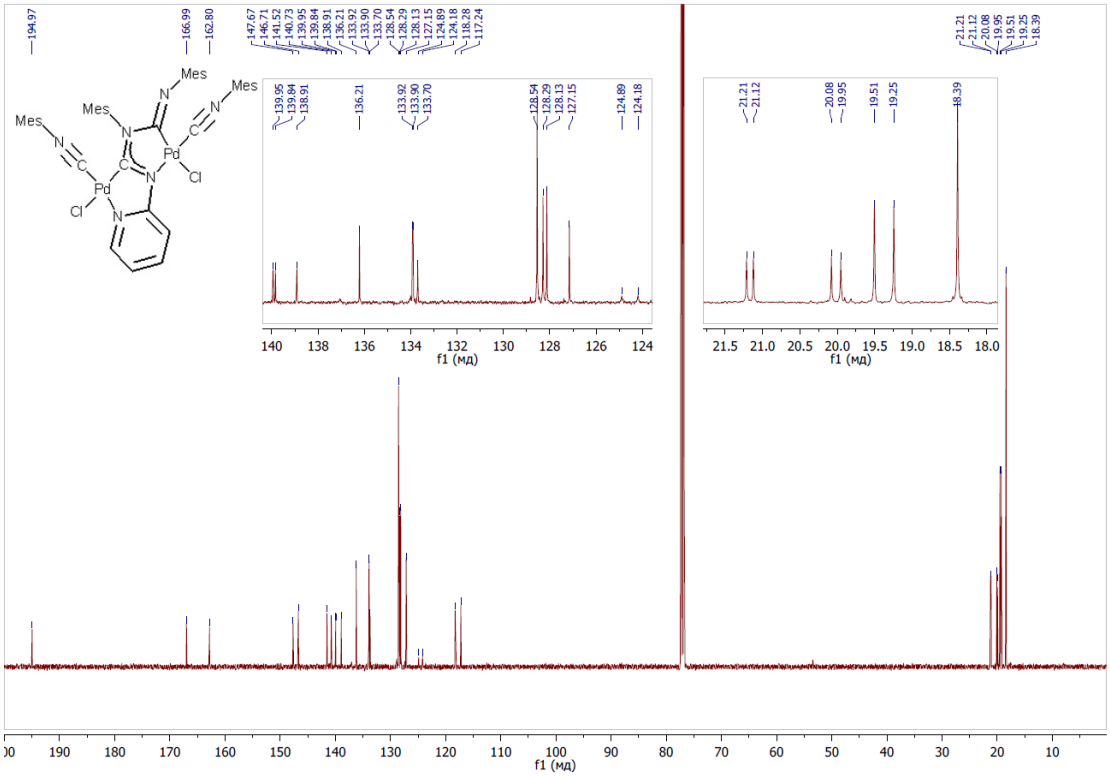

Figure S21. The ^{13}C{^{1}H} NMR spectra of **9**.

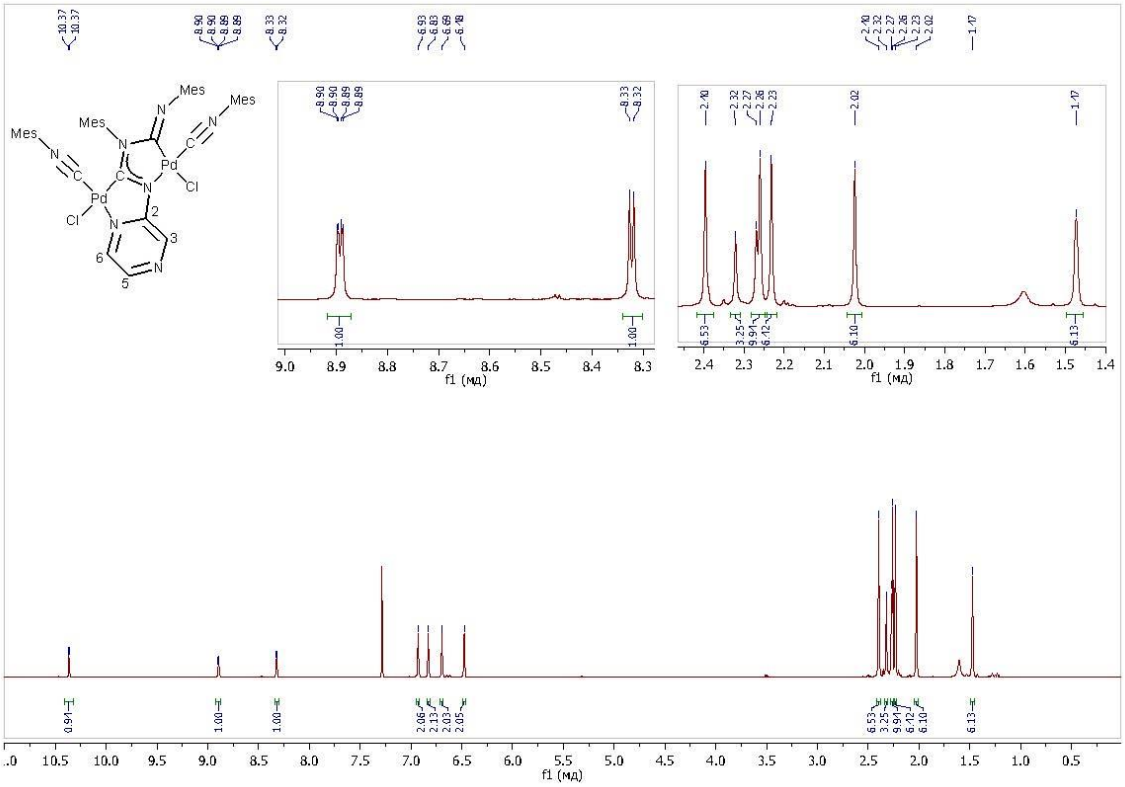

Figure S22. The ^{1}H NMR spectra of **10**.

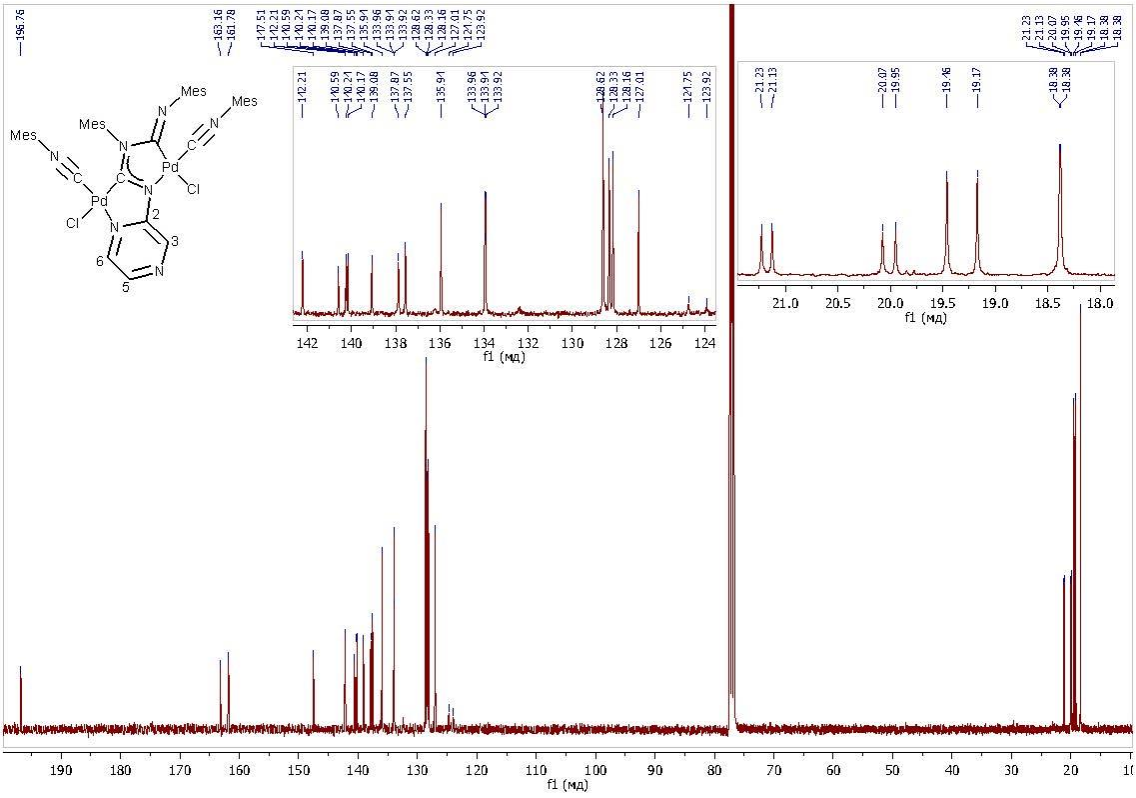

Figure S23. The $^{13}C\{^{1}H\}$ NMR spectra of **10**.

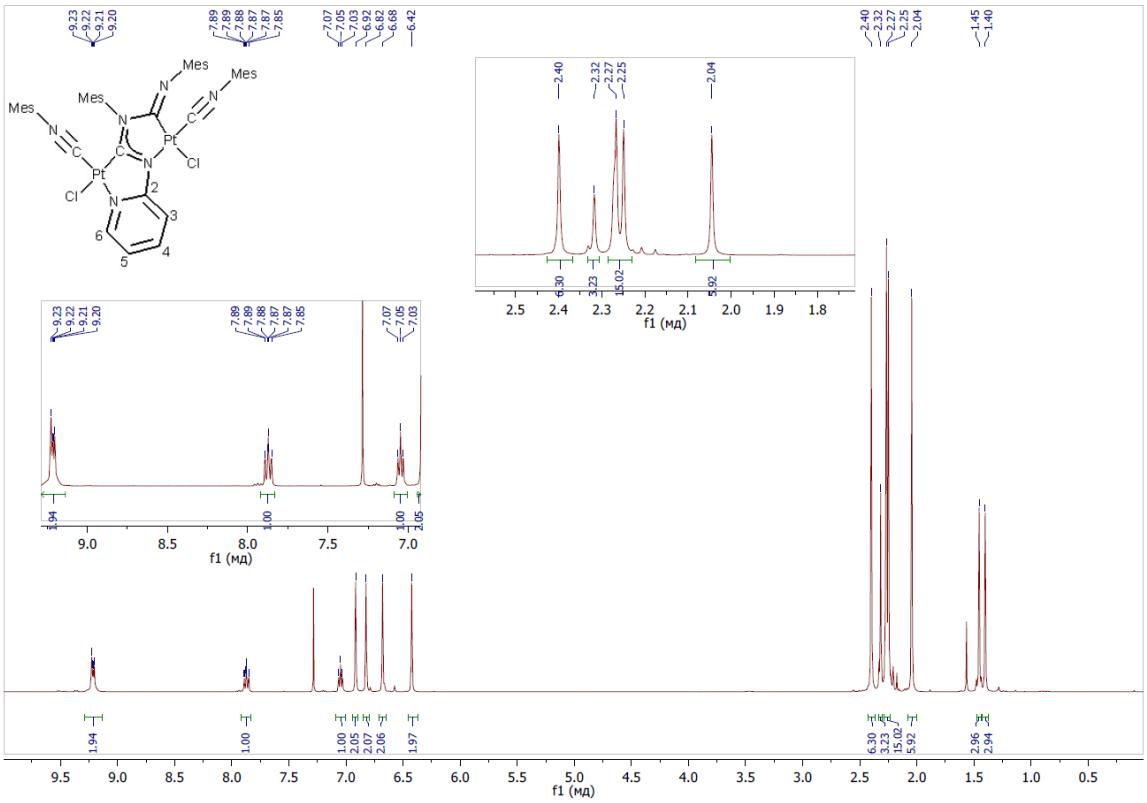

Figure S24. The ^{1}H NMR spectra of **11**.

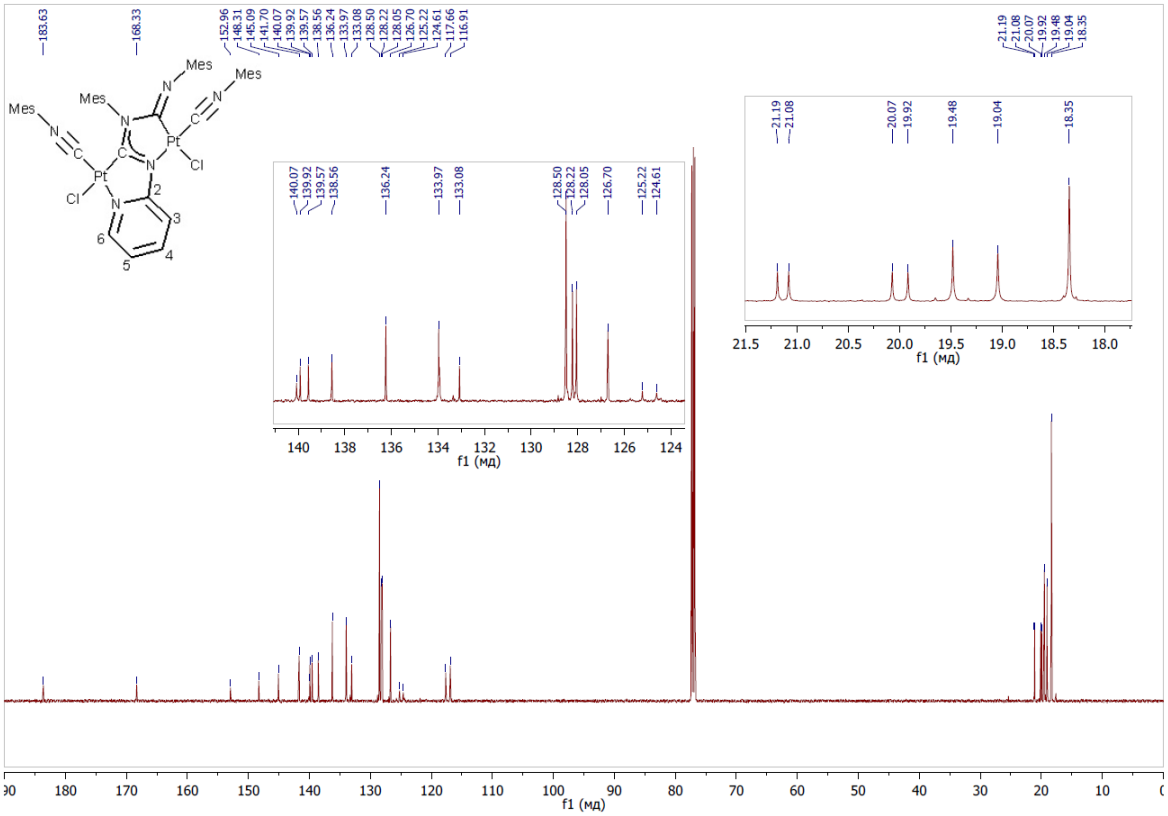

Figure S25. The ^{13}C{^{1}H} NMR spectra of **11**.

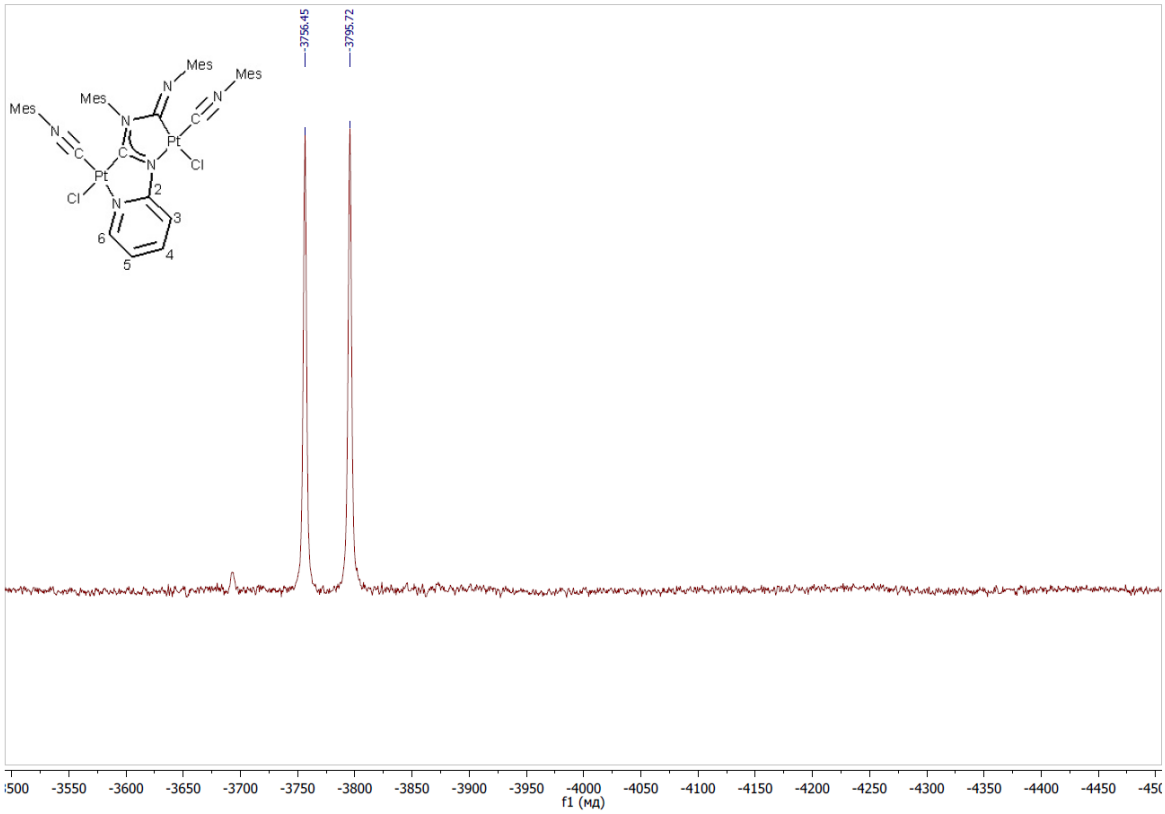

Figure S26. The $^{195}Pt\{^{1}H\}$ NMR spectra of **11**.

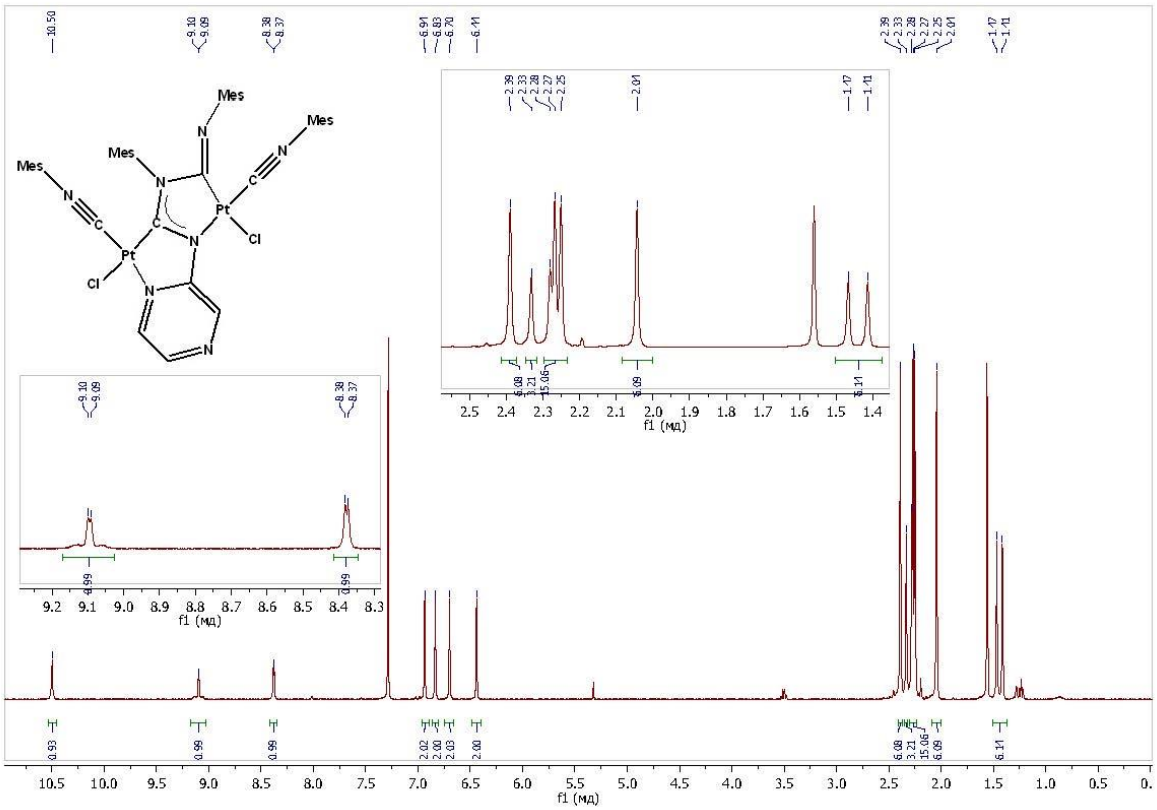

Figure S27. The ^{1}H NMR spectra of **12**.

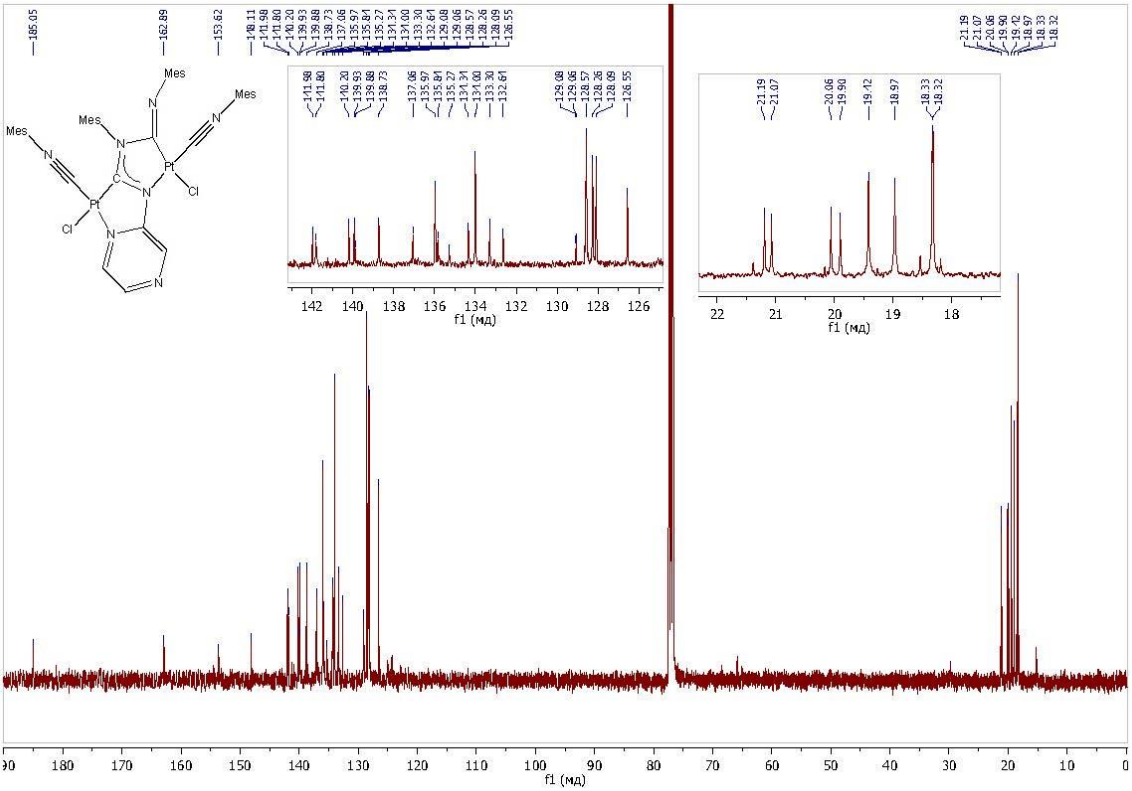

Figure S28. The $^{13}C\{^{1}H\}$ NMR spectra of **12**.

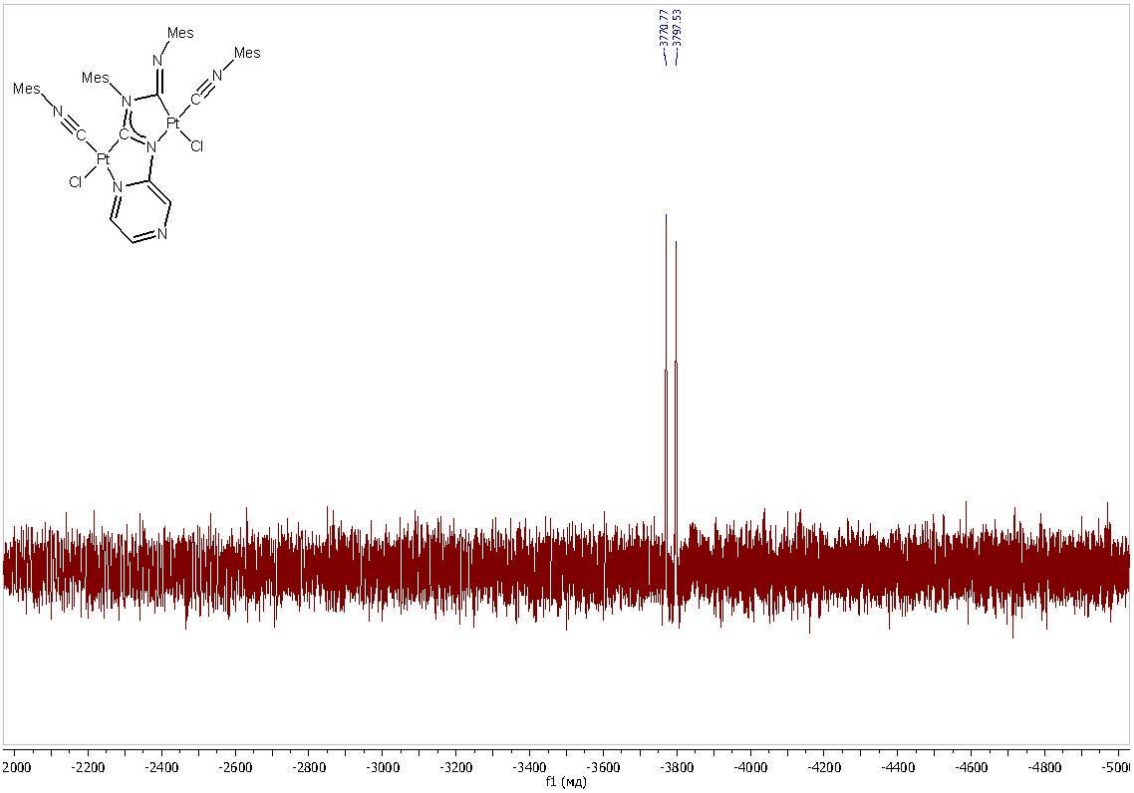

Figure S29. The $^{195}Pt\{^{1}H\}$ NMR spectra of **12**.

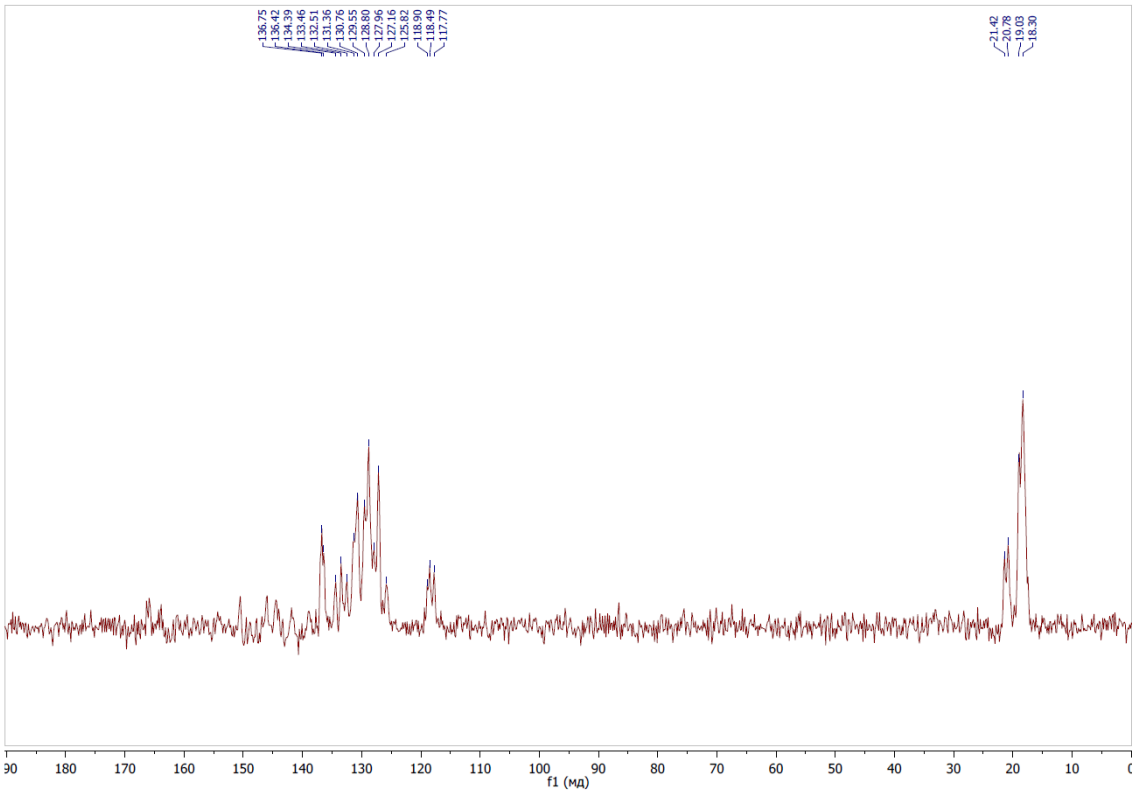

Figure S30. The ^{13}C CP/MAS NMR spectra of **13**.

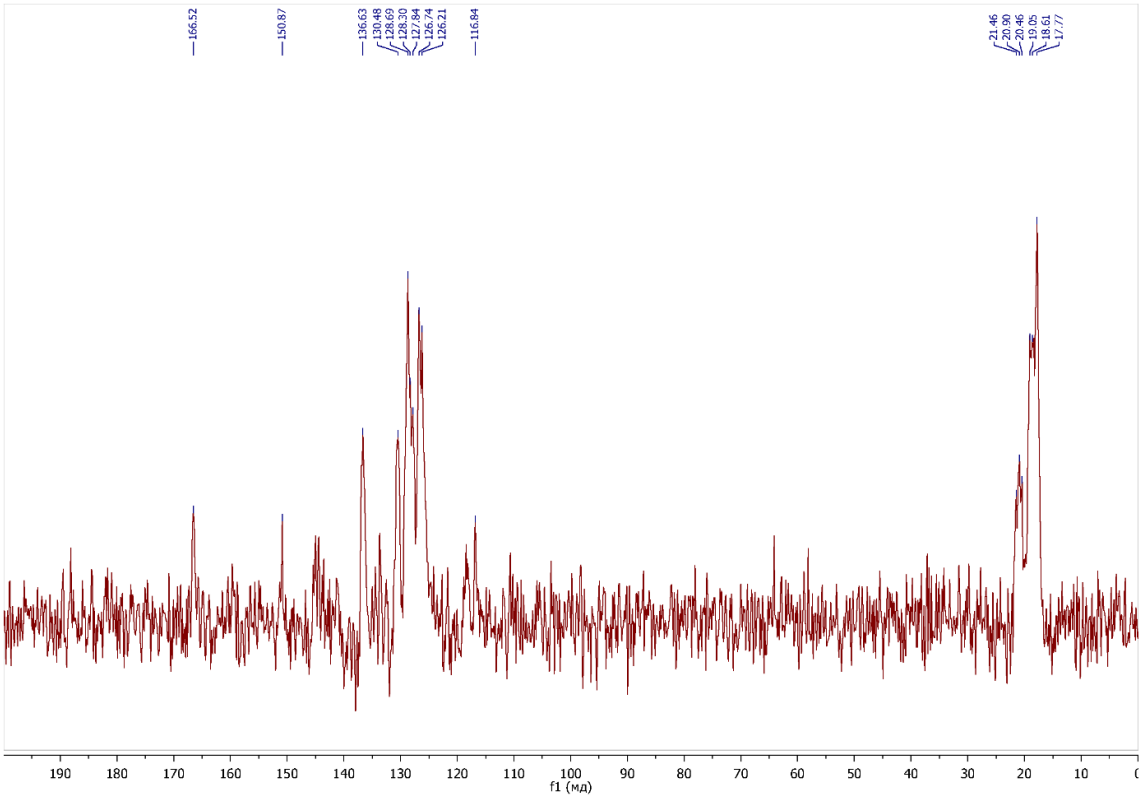

Figure S31. The ^{13}C CP/MAS NMR spectra of **14**.

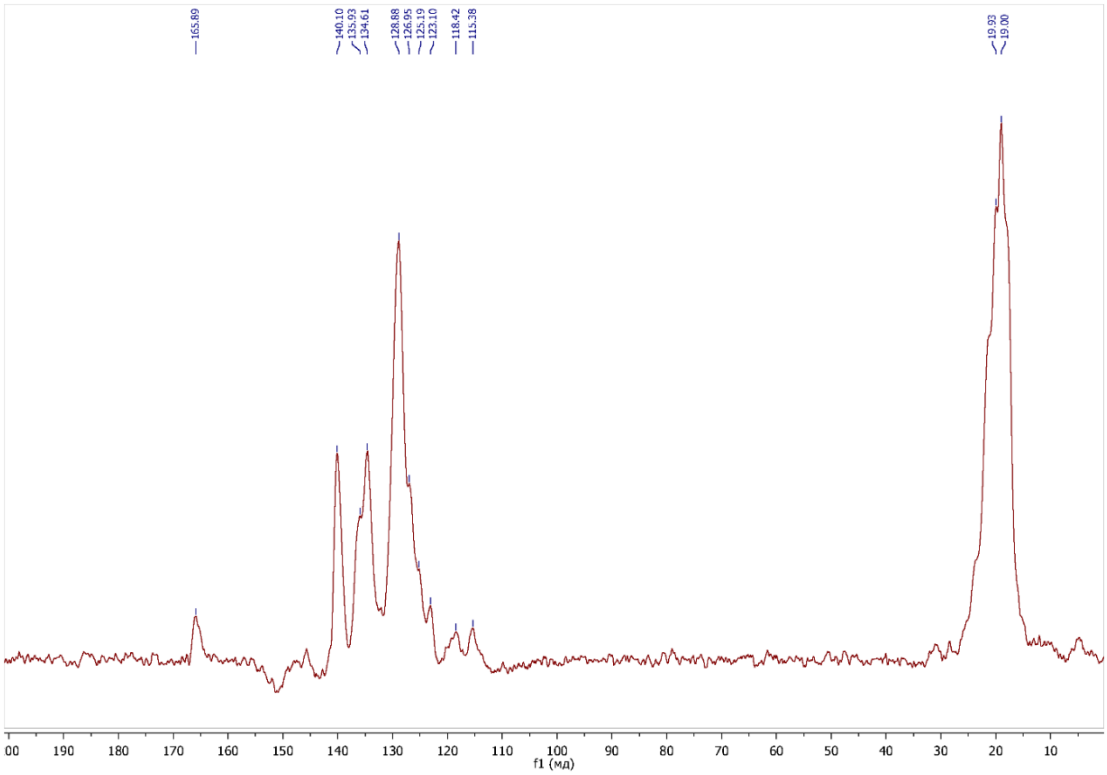

Figure S32. The ^{13}C CP/MAS NMR spectra of **15**.

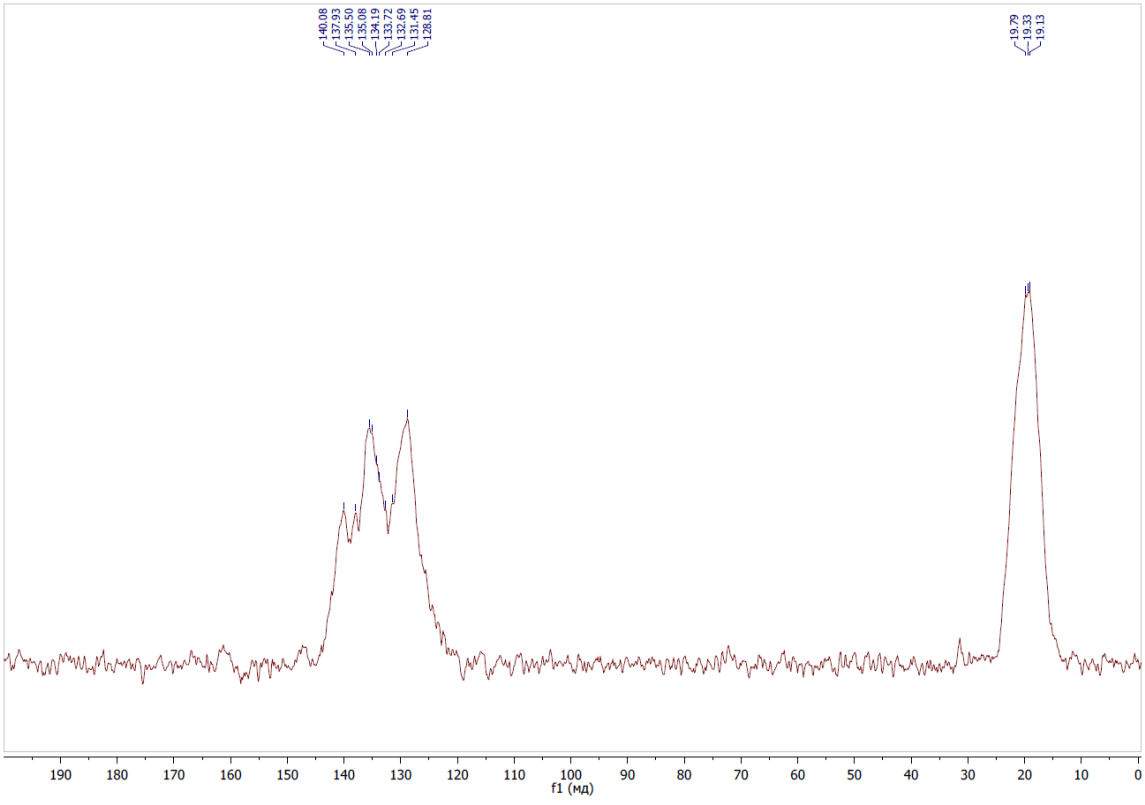

Figure S33. The ^{13}C CP/MAS NMR spectra of **16**.

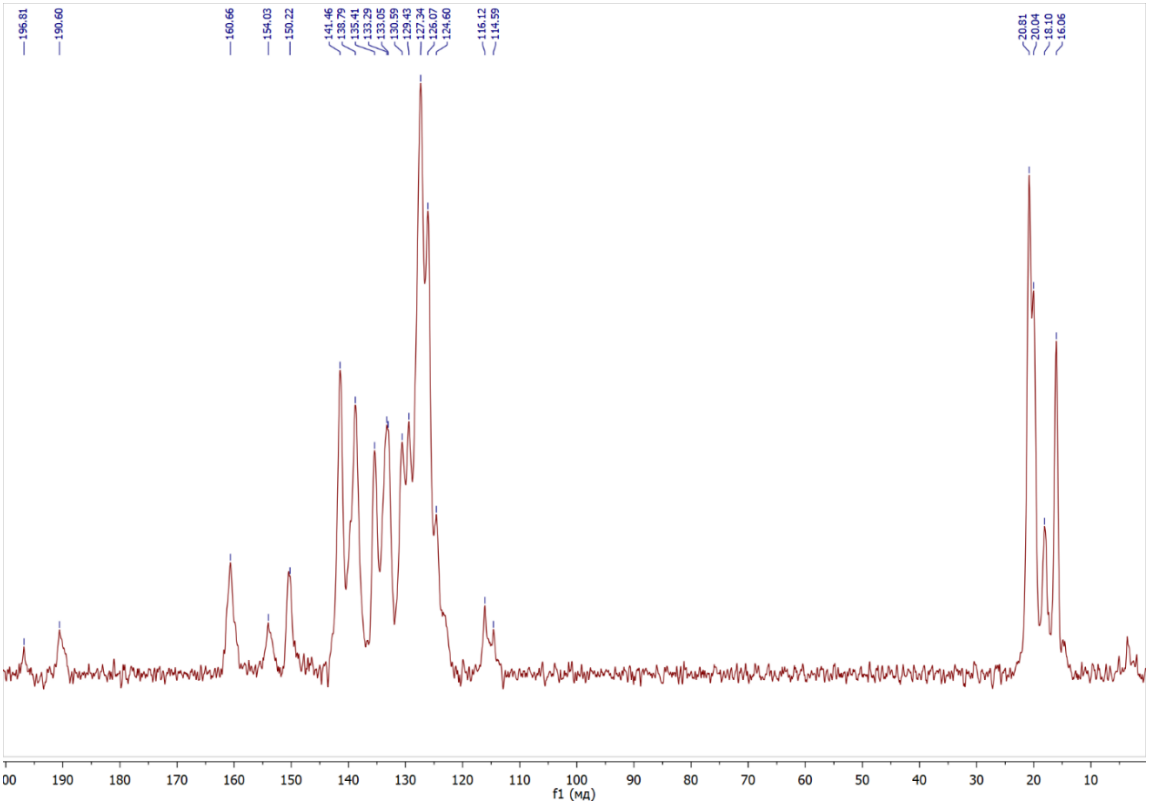

Figure S34. The ^{13}C CP/MAS NMR spectra of **17**.

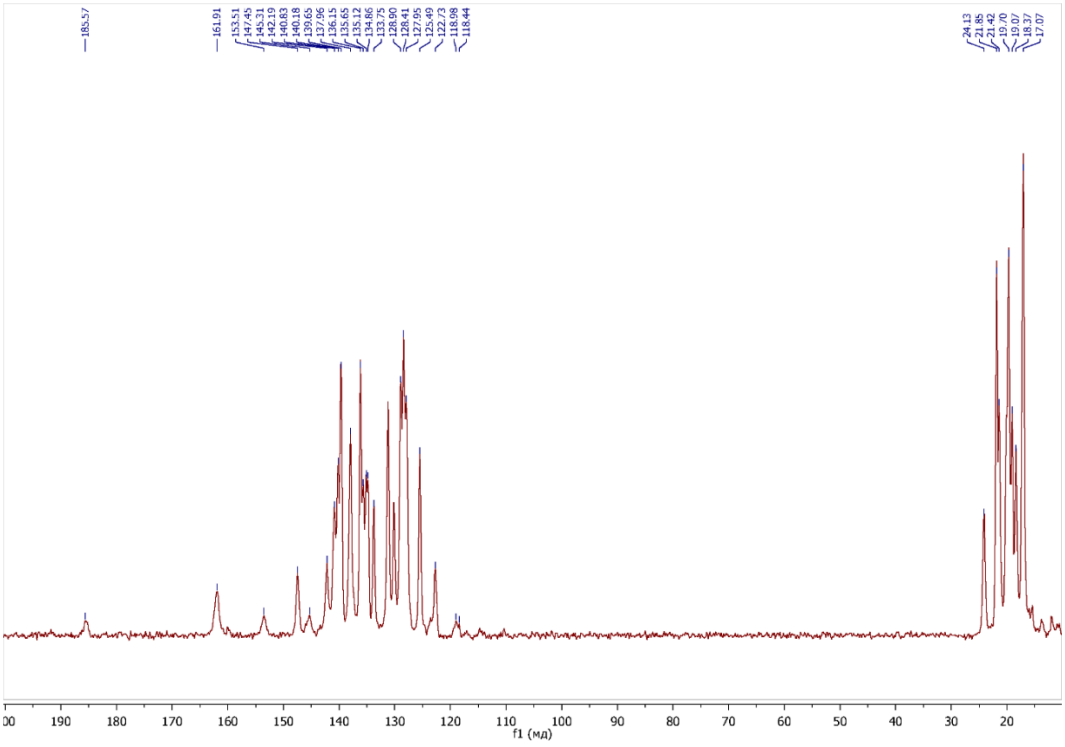

Figure S35. The ^{13}C CP/MAS NMR spectra of **18**.

S8. FTIR spectra for complexes **9**–**18**

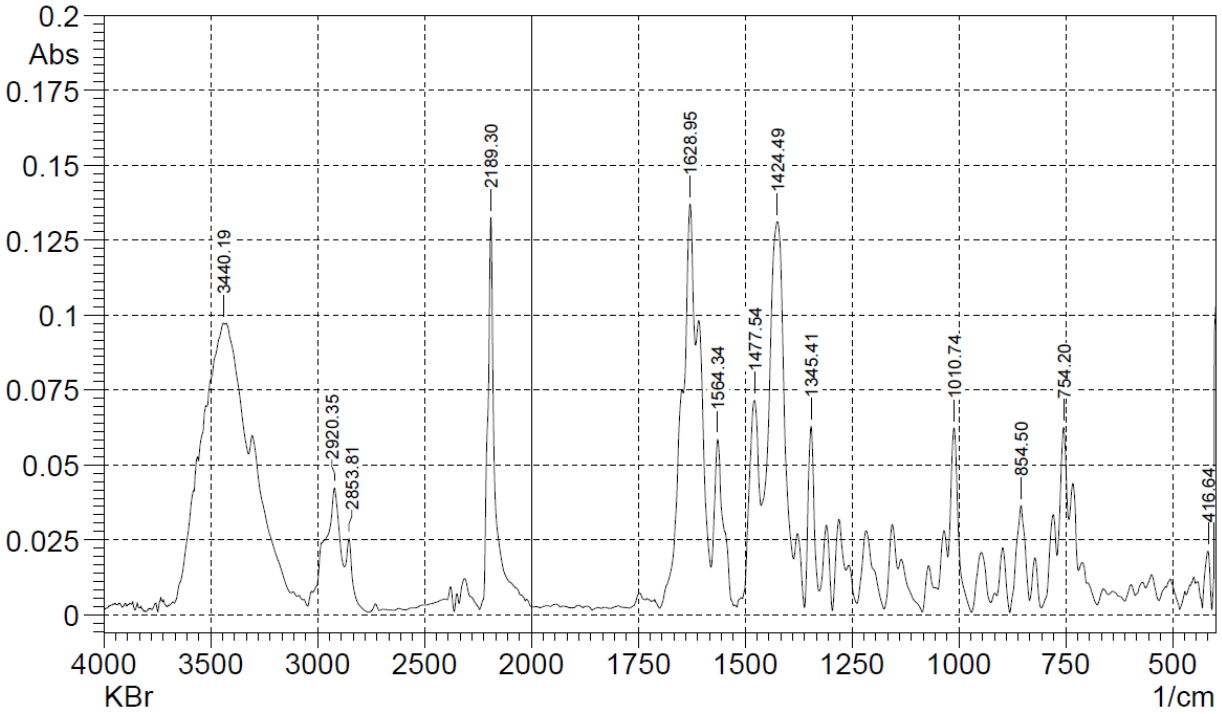

Figure S36. The FTIR spectra of **9**.

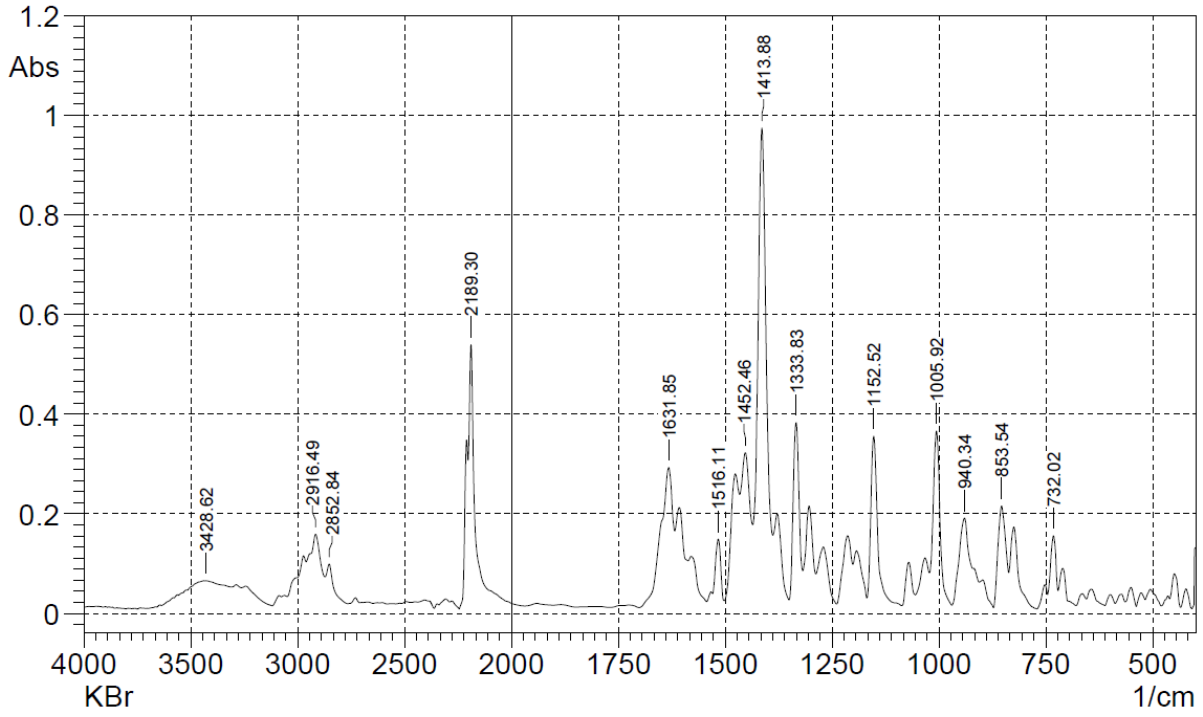

Figure S37. The FTIR spectra of **10**.

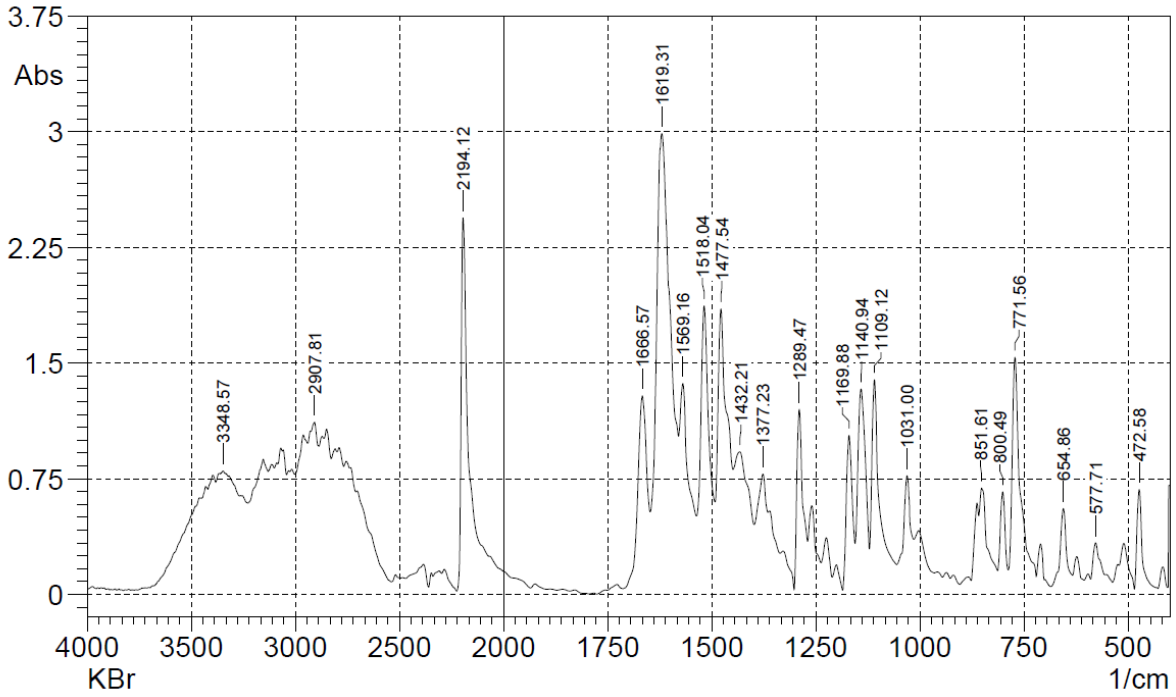

Figure S38. The FTIR spectra of **11**.

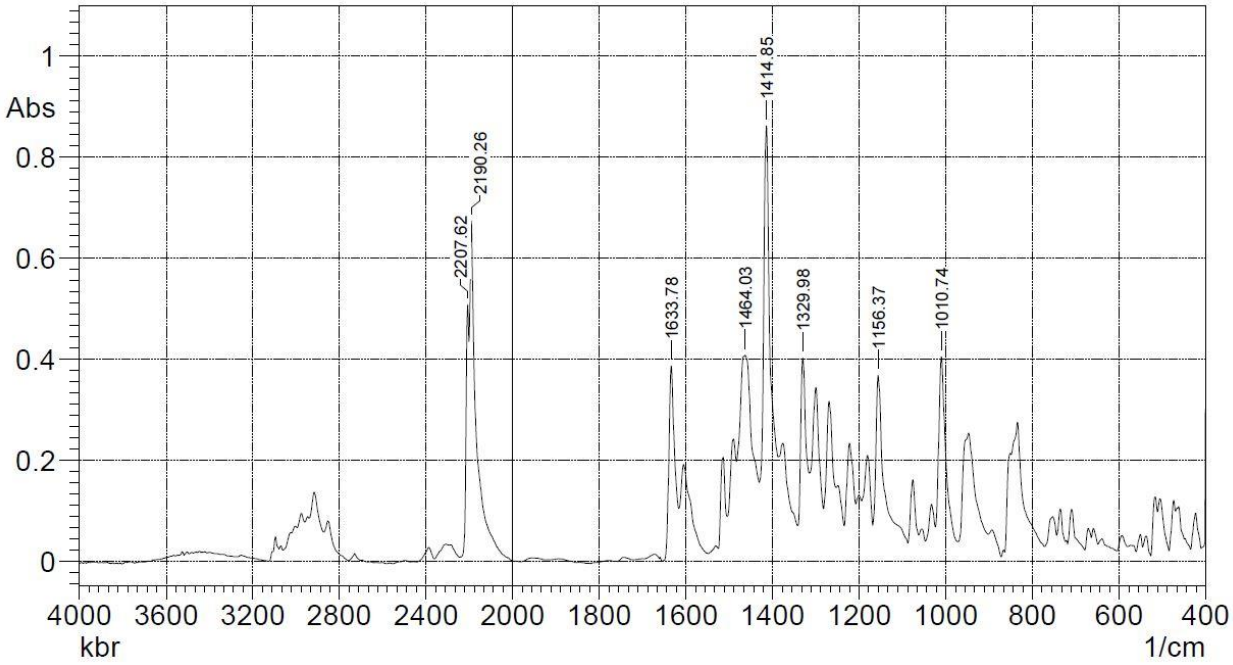

Figure S39. The FTIR spectra of **12**.

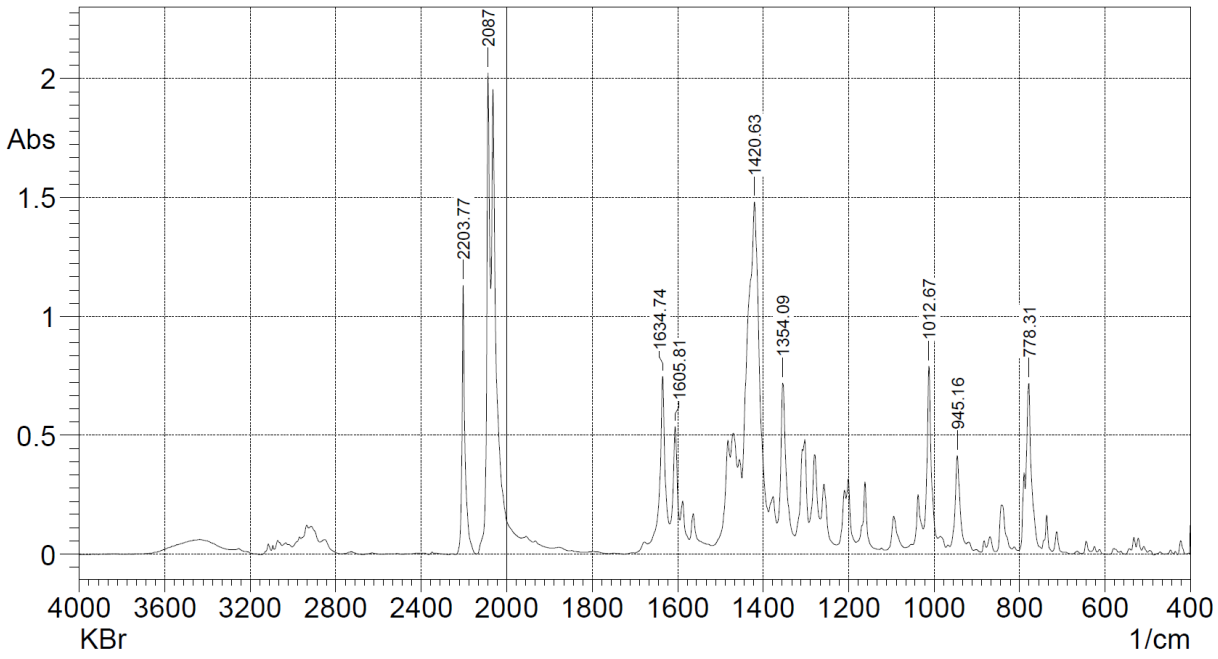

Figure S40. The FTIR spectra of **13**.

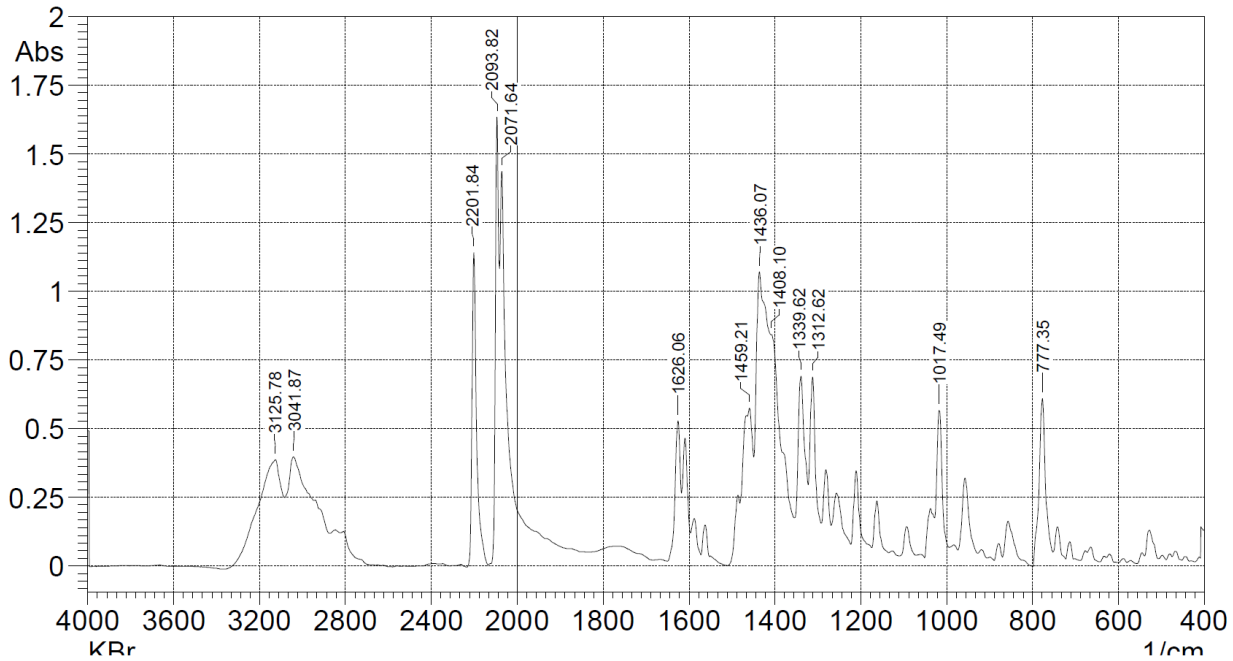

Figure S41. The FTIR spectra of **14**.

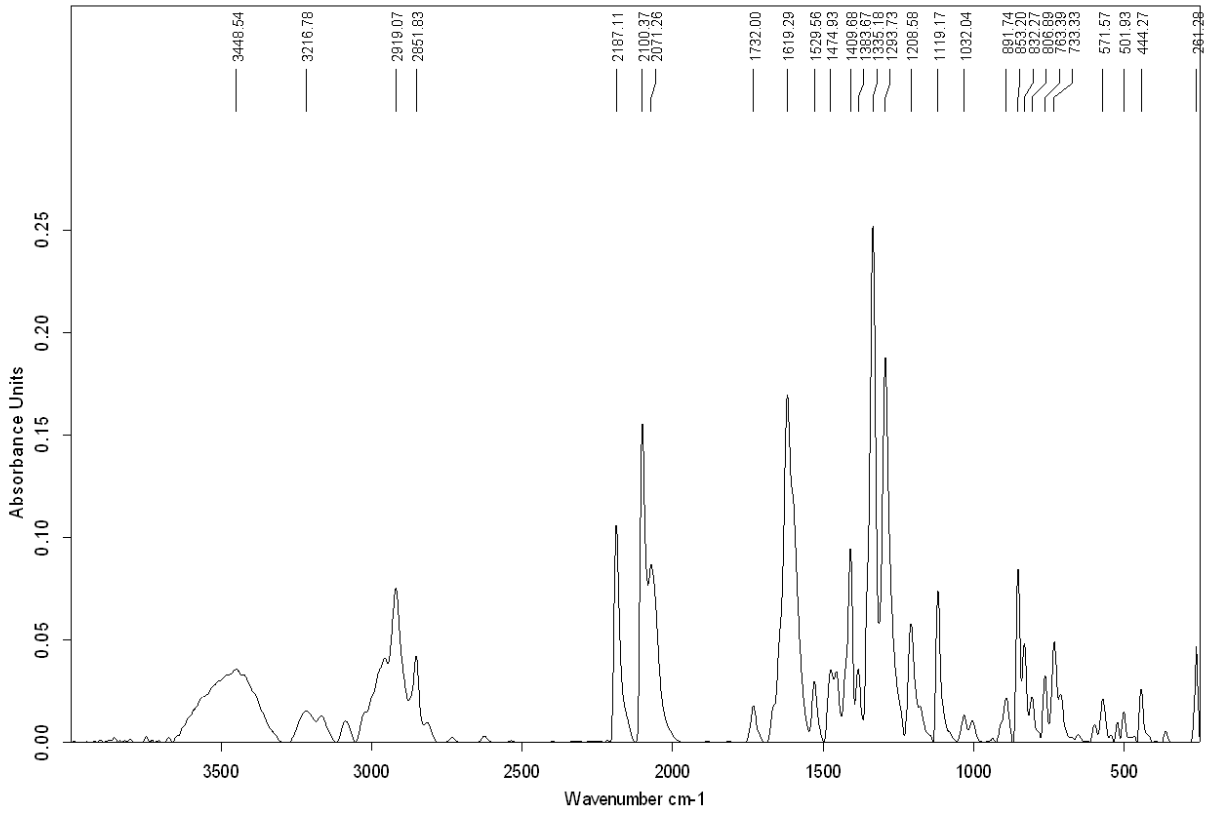

Figure S42. The FTIR spectra of **15**.

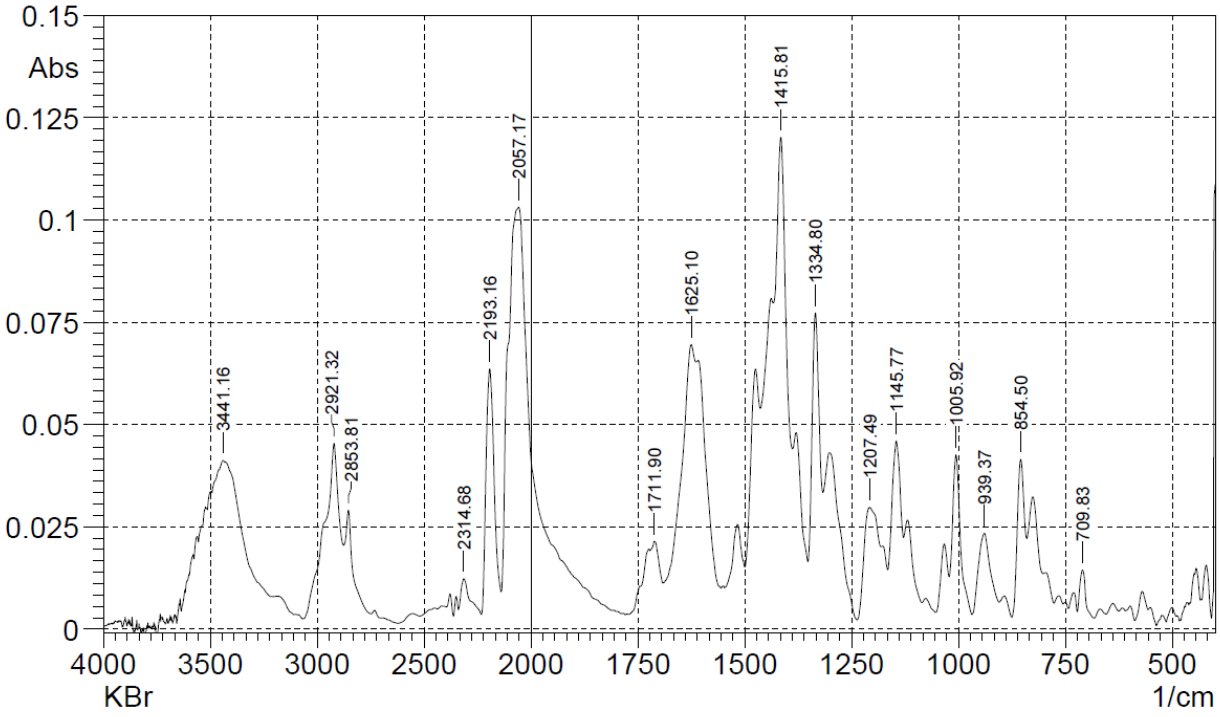

Figure S43. The FTIR spectra of **16**.

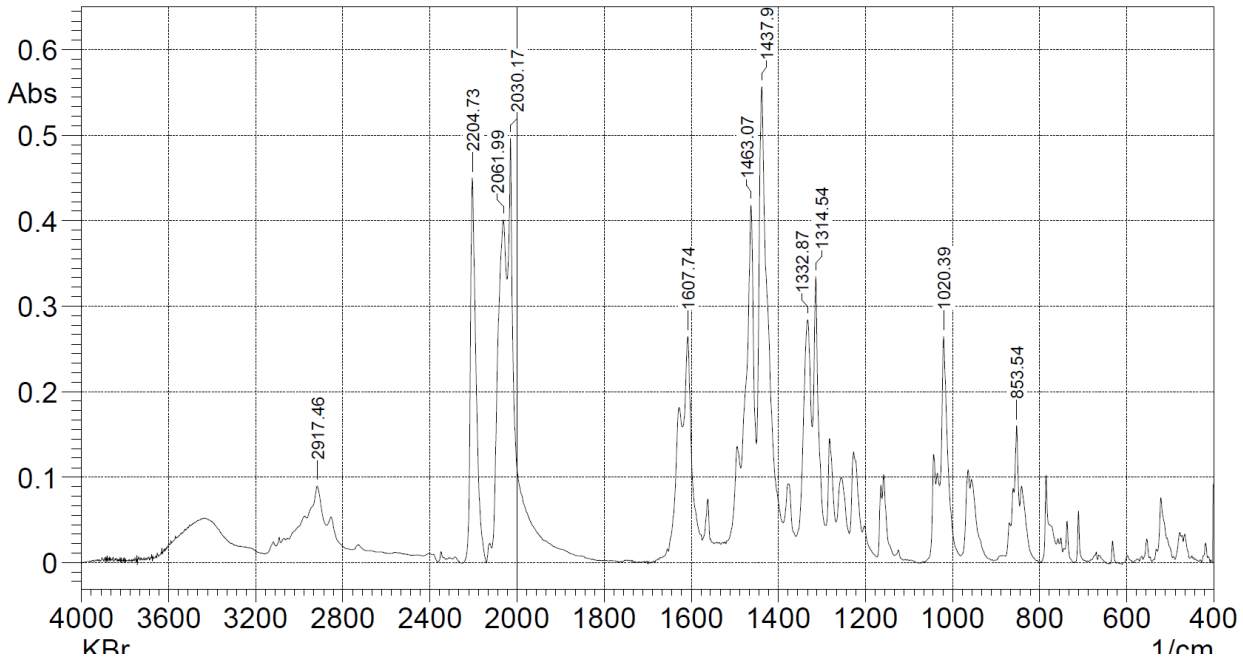

Figure S44. The FTIR spectra of **17**.

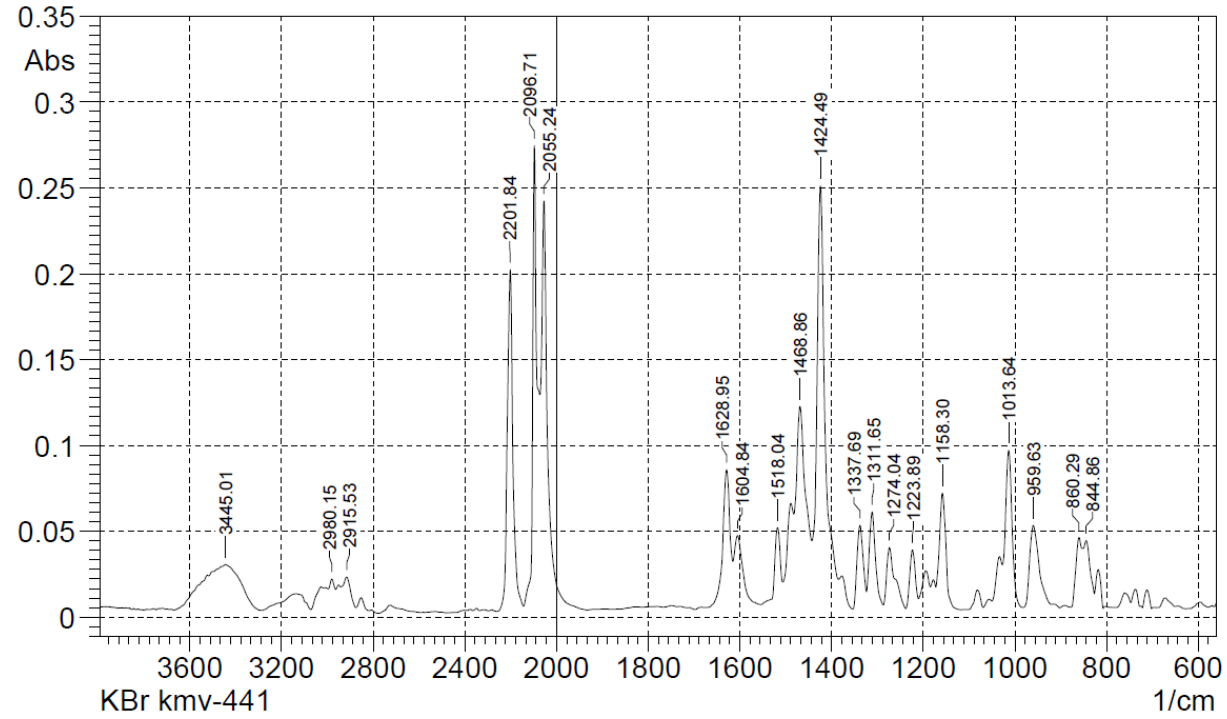

Figure S45. The FTIR spectra of **18**.

S9 References

1. (a) A. S. Novikov and M. L. Kuznetsov, Theoretical study of Re(IV) and Ru(II) bis-isocyanide complexes and their reactivity in cycloaddition reactions with nitrones, *Inorganica Chim. Acta*, 2012, **380**, 78; (b) A. A. Melekhova, A. S. Novikov, T. L. Panikorovskii, N. A. Bokach and V. Y. Kukushkin, A novel family of homoleptic copper(i) complexes featuring disubstituted cyanamides: a combined synthetic, structural, and theoretical study, *New J. Chem.*, 2017, **41**, 14557.
2. E. D. Glendening, C. R. Landis and F. Weinhold, Natural bond orbital methods, *Wiley Interdiscip. Rev. Comput. Mol. Sci.*, 2012, **2**, 1.
3. I. Mayer and P. Salvador, Overlap populations, bond orders and valences for 'fuzzy' atoms, *Chem. Phys. Lett.*, 2004, **383**, 368.
4. A. E. Reed, L. A. Curtiss and F. Weinhold, Intermolecular interactions from a natural bond orbital, donor-acceptor viewpoint, *Chem. Rev.*, 1988, **88**, 899.
5. S. Dapprich and G. Frenking, Investigation of Donor-Acceptor Interactions: A Charge Decomposition Analysis Using Fragment Molecular Orbitals, *J. Phys. Chem.*, 1995, **99**, 9352.
6. S. I. Gorelsky, S. Ghosh and E. I. Solomon, Mechanism of N2O Reduction by the μ4-S Tetranuclear CuZ Cluster of Nitrous Oxide Reductase, *J. Am. Chem. Soc.*, 2006, **128**, 278.
7. F. H. Allen, O. Kennard, D. G. Watson, L. Brammer, A. G. Orpen and R. Taylor, Tables of bond lengths determined by X-ray and neutron diffraction. Part 1. Bond lengths in organic compounds, *J. Chem. Soc., Perkin Trans. 2*, 1987, **0**, S1.
8. (a) K. Ha, (2,2'-Bipyrimidine-$\kappa^2N^1,N1'$)bis(thiocyanato-κN)platinum(II), *Acta Crystallogr. E*, 2012, **68**, m676; (b) S. Paziresh, R. Babadi Aghakhanpour, S. Fuertes, V. Sicilia, F. Niroomand Hosseini and S. M. Nabavizadeh, A double rollover cycloplatinated(ii) skeleton: a versatile platform for tuning emission by chelating and non-chelating ancillary ligand systems, *Dalton Trans.*, 2019, **48**, 5713; (c) K. Ha, Crystal structure of (1,10-phenanthroline-κ2N,N′)bis(thiocyanato-κN)platinum(II), $C_{14}H_8N_4PtS_2$, *Z. Kristallogr. NCS*, 2016, **231**, 329; (d) A. J. Paviglianiti, D. J. Minn, W. C. Fultz and J. L. Burmeister, The conjunctive response to steric hindrance in dithiocyanato[bis(diphenylphosphino)alkyl or aryl]palladium(II) complexes: a new look at a classic series, *Inorganica Chim. Acta*, 1989, **159**, 65; (e) A. D. Yeung, P. S. Ng and H. V. Huynh, Co-ligand effects in the catalytic activity of Pd(II)–NHC complexes, *J. Org. Chem.*, 2011, **696**, 112.